AD-A131 841 GROWTH AND CHARACTERIZATION OF INP AND INGAAS FILMS USING TH$ HYDRIDE VPE TECHNIQUE(U) COLORADO STATE UNIV FORT COLLINS DEPT OF ELECTRICAL ENGINEERI.. 21 OCT 82 1/1

UNCLASSIFIED N00019-81-C-0425 F/G 20/12 NL

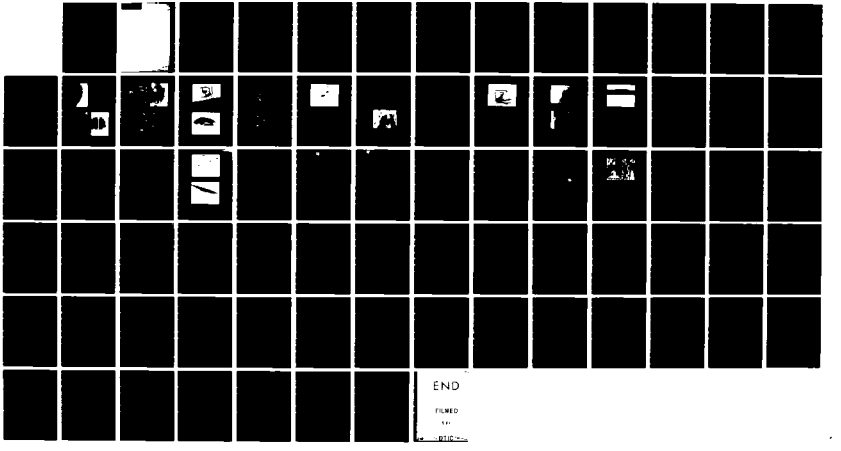

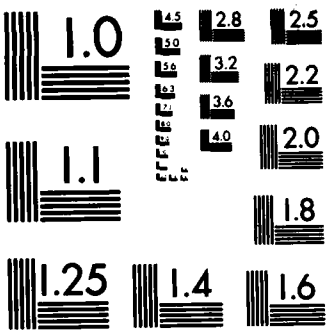

MICROCOPY RESOLUTION TEST CHART
NATIONAL BUREAU OF STANDARDS-1963-A

AD A131841

TABLE OF CONTENTS

		Page
	Abstract	1
I	Introduction	3
II	Growth and Characterization	6
	A. Refinements in the Growth System	6
	B. Growth of the InP Using Cylinder HCl	6
	1. Experimental Procedure	6
	2. Results	7
	a. Morphology	7
	b. Carrier Concentration and Mobility	15
	3. Discussion	15
	a. Morphology and Growth Rate	15
	b. Carrier Concentration and Mobility	20
	c. Growth of InP Using HCl from PCl_3	21
	C. Growth of InGaAs Films	23
	D. Surface Studies	29
	1. Experimental Procedure	29
	2. Results	30
	3. Discussion	34
	4. Effects of Downstream HCl Etch	34
III	Theoretical Studies	35
	A. Hydride and Chloride Comparison	35
	1. Physical Analysis	35
	2. Mathematical Analysis	39
	3. Results	46
	a. Source Zone	46
	b. HCl Concentration	48
	c. Growth Rate	55
	B. Thermodynamic Effects of Using an Inert Gas	60
	References	68

APPROVED FOR PUBLIC RELEASE
DISTRIBUTION UNLIMITED

LIST OF FIGURES

1. Photomicrographs of films grown with III/V ratios of a.) .25/1.5 (37.5x), b.) .5/1.5 (37.5x), c.) 1.0/1.5 (37.5x), and d.) 1.0/1.5 (300x) ---- 9

2. Photomicrographs of films grown with III/V ratios of a.) 1.5/1.5 (37.5x), b.) 3.0/1.5 (37.5x), and c.) 4.0/1.5 (37.5x) ---- 10

3. Scanning electron micrographs of films grown with III/V ratios of a.) .25/1.5 (215x) and b.) 4.0/1.5 (360x) ---- 11

LIST OF FIGURES - Continued

Page

4. Photomicrographs of films grown with III/V ratios of a.) 1.0/2.0 (37.5x), and b.) .5/6 (37.5x)---------- 12

5. Scanning electron micrograph of a film grown with III/V ratio of 1.0/2.0 (575x)---------- 13

6. Photomicrographs of films grown with III/V ratios of a.) .25/.50 (37.5x), b.) .5/1.0 (37.5x)---------- 14

7. A scanning electron micrograph of a film grown with a III/V ratio of .5/1.0---------- 16

8. Photomicrographs of films grown with III/V ratios of .25/.50 at a.) 600 (37.5x), and b.) 700°C (37.5x)---------- 17

9. A scanning electron micrograph of a film grown with a III/V ratio of .25/.50 at 700°C---------- 18

10. A schematic diagram of the cracking furnace---------- 22

11. Morphology of an InGaAs film a.) 214x and b.) 2140x---------- 25

12. a.) Rocking curves for InGaAs films grown on InP substrates preheated in PH_3 or AsH_3, b.) K_{α_1} and K_{α_2} peaks for an InP substrate, c.) Rocking curve for an InGaAs film lattice matched to within .5% of the InP substrate---------- 27,28

13. Photomicrographs of a.) a substrate exposed to H_2 only for 30 min. at 650°C (37.5x) and b.) a partially covered substrate bathed in PH_3 at 1.5×10^{-2} atm. for 30 min. at 650°C (37.5x)---------- 31

14. A scanning electron micrograph of a substrate exposed to H_2 for 30 min. at 650°C (1440x)---------- 32

15. The transient behavior of the formation of the InP crust in the chloride system. a.) More phosphorus is reacting with the liquid indium than is being generated by the attack of InP by HCl; b.) more than 2/3 of the HCl is reacting with the liquid indium; c.) the steady state condition when the same amount of phosphorus is being generated as is reacting, and ∿2/3 of the HCl is reacting with the liquid indium and ∿1/3 of it is reacting with the InP---------- 38

16. The nomenclature used to designate the source (a) and deposition zone (b) input and output constituents---------- 40

LIST OF FIGURES - Continued

Page

17. The fraction, u, of phosphorus consumed by the reaction with liquid indium, and the fraction, v, of the InP consumed by the reaction with HCl plotted as a function of source input PCl_3---------- 47

18. The deposition zone equilibrium constitutent partial pressures plotted as a function of the z.) HCl, b.) PH_3, and c.) PCl_3 input pressures---------- 49-51

19. The equilibrium HCl concentration plotted as a function of downstream HCl/3 or PCl_3, when the input HCl/3 (——), PH_3 (---), or PCl_3(...) pressure equals .01/3, .01, and .03 atm.---------- 54

20. The normalized ideal growth rate plotted as a function of input HCl/3, PH_3 and PCl_3 pressures---------- 56

21. The normalized ideal growth rate plotted as a function of downstream HCl/3 or PCl_3 input pressures when the input HCl/3, PH_3 or PCl_3 pressure equals .01/3, .01, and .03 atm.--- 59

22. The equilibrium partial pressures of HCl, PH_3, P_2, P_4, InCl, and H_2 in the deposition zone plotted as a function of I_I when P_{HCl^o} and $P_{PH_3^o}$ = .01 atm., T_s = 750°C, and T_D = 650°C---------- 64

23. The thermodynamic growth rate plotted as a function of P_I when the $P_{HCl^o}/P_{PH_3^o}$ ratio is .01/3/.01, .01/.01, .03/.01, .01/.01/3 or .01/.03 and when T_D = 600 and 700°C---------- 65

LIST OF TABLES

1. Room temperature and liquid nitrogen carrier concentrations and mobilities and growth rate for some InP films---------- 19

2. Room temperature carrier concentration and mobility and growth rate for InGaAs films grown under a variety of In/Ga and III/V ratios---------- 29

3. The qualitative results of an ESCA analysis of the surface of a substrate subjected to different environments at 650°C for 15 minutes---------- 33

LIST OF TABLES - Continued

Page

4. The range of HCl pressures x 10^3 in the deposition zone generated by introducing HCl or PCl_3 downstream at a concentration of 0 and the point where etching begins for input HCl/3, PH_3 or PCl_3 pressures of .01/3, .01, and .03 atms.---------- 57

5. The HCl^2/HCl^o, $HCl^2/3/PH_3^2$ and PCl_3^2/PCl_3^o ratios at the concentration where etching begins for input HCl/3, PH_3 or PCl_3 pressures of .01/3, .01, and .03 atms.---------- 57

6. The HCl and PH_3 partial pressures for different values of P_I for standard conditions, when P_{HCl^o} or $P_{PH_3^o}$ = .01/3 or .03 atm., or when T_D = 600 or 700°C---------- 67

Accession For
NTIS GRA&I
DTIC TAB
Unannounced
Justification
Distribution/
Availability Codes
Dist
A

ABSTRACT

The advantages of the hydride growth technique are that the control is good because the anion and cation concentrations are separately controlled, and it can be easily scaled up. The disadvantages are that the films tend to have a higher background carrier concentration and a more rough morphology. The focus of this research was to find ways to mitigate or possibly eliminate these disadvantages.

An in-depth theoretical comparison between the chloride and hydride growth techniques showed that hydride growth is thermodynamically similar to steady state chloride growth when the $HCl:PH_3$ ratio is 3:1. If chloride systems are inherently cleaner than hydride systems it is possibly due to the cleansing reaction of the phosphorus with the liquid indium to form InP with a subsequent attack of the InP by HCl.

However, it seems more likely that the source of the higher carrier concentration is due to the less pure HCl used. We showed this by growing lower carrier concentration InP films when we used HCl generated from ultrapure PCl_3.

Another possible impurity source is silicon from the silica reactor. It has been suggested that this contamination source can be reduced by increasing the deposition zone HCl concentration. We attempted to do this by introducing HCl downstream. However, we found that the HCl concentration is not increased much by doing this because it retards the deposition reaction.

A more important effect of using downstream HCl is that it greatly improves the morphology when it is used during the preheat treatment. This procedure also reduces the carrier concentration. It is clear that the substrate surface preheat treatment strongly affects the film quality. We will focus our research on this problem during the next year.

The preheat treatment also greatly affected the quality of our InGaAs films. The rocking curve peak widths were smallest when a downstream HCl etch was used, were larger when the substrate was bathed in AsH_3 during the five minute warm-up period, and were largest when the substrate was bathed in PH_3 during the warm-up. We will study these effects in more detail next year.

We found that our InGaAs films were most closely lattice matched at our growth temperature of 700°C when the HCl(In)/HCl(Ga) ratio was 7:1 and the III/V ratio was 1.75:1. We plan to study the effects of lattice mismatch in more detail next year.

GROWTH OF InP AND InGaAs FILMS USING THE HYDRIDE VPE TECHNIQUE

I. Introduction

When compared to the other growth methods, the hydride VPE method has a number of advantages [1]. More control can be exercised using this method than with the chloride VPE method in that indium and phosphorus concentrations are independently controlled, and growth of the quarternaries is less complex in that two source zones are required whereas three are required for the chloride system [2]. Indium containing complexes form under normal operating conditions in a metalorganic VPE system [3], and there is also a problem with carbon contamination. The molecular beam epitaxy technique [4] is not a viable economic alternative for a number of applications. Liquid phase epitaxial systems cannot be as completely controlled in that it is difficult to grade the doping composition, and the film is always grown in a cation rich environment. Also, the morphology is much more sensitive to the lattice mismatch [5]. In addition to the advantages enumerated above, the hydride technique can easily be scaled up.

The primary disadvantages of the hydride technique are that the control is more difficult to maintain, the background carrier concentration is relatively high, and it is more difficult to grow films with a smooth morphology. Control is more difficult since, even for the binaries, the degree of supersaturation is determined by the constituent partial pressures as well as the deposition zone temperature, whereas in the chloride system it is controlled only by the temperature difference between the source and deposition zones. The lowest background carrier concentration for hydride grown InP films are typically 10^{15} cm^{-3} and the 77K mobilities

are ~50,000 $cm^2\ V^{-1}\ s^{-1}$ [6], whereas the corresponding values for chloride grown films are $<10^{14}\ cm^{-3}$ [7,8] and ~100,000 $cm^2\ V^{-1}\ s^{-1}$ [7]. Similar differences also exist for GaAs films grown by the two techniques [9,10].

Because the background carrier concentration is not usually an important parameter for light emitting and detecting devices, they have been successfully fabricated from hydride grown InGaAs [11] and InGaAsP [12] films. However, there is now interest in growing low carrier concentration InGaAs films for high speed detectors using the hydride technique [11]. There is also an interest in growing low carrier concentration InP films to be used as buffer layers for InGaAs FET's [13]. Further, low carrier concentration InP films are needed for high speed low noise TED's [14].

In trying to find the source of the background carrier concentration, we first made certain that we had a tight system. Then we analyzed the chloride and hydride systems to determine how they differ, and to try to understand how these differences can account for the difference in the background carrier concentration. The analysis included computing the equilibrium partial pressures in the hydride source zone, the steady state partial pressures in the chloride source zone, the equilibrium partial pressures in the deposition zone of both systems, and the ideal growth rate of both systems. Based on these computations, films were grown in our hydride growth system under conditions which best matched those in the chloride system.

One primary difference between the chloride and the hydride growth systems is that in the hydride system the HCl source is bottled HCl that flows through stainless steel tubing to the source zone, whereas HCl is a reaction product between PCl_3 and H_2 in the chloride system. It is

possible that the source of the higher background carrier concentration in the hydride system is the less pure HCl from the gas cylinder which also might react with the stainless steel tubing on the way to the source zone. We studied this possibility by generating HCl from PCl_3 and using it in our hydride growth system.

Another possible source of impurities is silicon contamination from the silica reactor. We tried to suppress this reaction by introducing HCl downstream, but we had to be careful not to introduce too much because it would change the deposition reaction to one of etching.

We also introduced HCl downstream while the substrate was warming up. Our aim was to etch the surface as rapidly as it became depleted in phosphorus, and to etch it slowly so that the surface remained smooth. Clearly, this is a necessary condition for growing smooth films. We also experimented with bathing the substrate in PH_3 or AsH_3 or placing it under a cover piece during the warm up to try to improve the morphology. The effects of varying the $HCl:PH_3$ ratio as well as their absolute pressures were studied too.

The focus of our future research will be on the interface defects at the InP/InGaAs interface. This will include growing high quality InP buffer layers to eliminate the substrate effects, providing a smooth InP surface for the deposition of InGaAs, and lattice matching InGaAs to InP. We considered the first problem when we studied the background carrier concentration and the second problem when we considered the morphology. We also studied how the composition of the solid is related to the composition of the vapor, and how the composition of the solid, as well as the heat treatment prior to deposition, affect the internal stresses in the films.

We were successful in lowering the background carrier concentration by using HCl generated from PCl_3, and therefore believe that one of the sources of the higher background carrier concentration is the less pure HCl from the gas cylinder. We were able to improve the morphology by using a downstream HCl etch. Using the downstream HCl etch also reduced the strain in the InGaAs films as determined by the x-ray rocking curves.

II. Growth and Characterization

A. Refinements in the Growth System

The magnetic loader was built and installed. A cylindrical magnetic core is attached to the quartz rod holding the specimen holder. The specimen can now be inserted from the forechamber into the growth zone by moving a current coil externally along the walls of the pyrex forechamber. As the specimen moves forward, it is guided by teflon spacers.

Gallium and indium boats were made with covers. The upstream end of the boat contains a sleeve into which a quartz HCl tube is inserted, and the downstream end contains a small opening through which the reactants escape. This should insure good contact between HCl and the liquid metals thus enhancing the probability that the reaction will go to completion. The H_2 flow mixed in with the HCl gas is also reduced to increase the residency time of the HCl over the liquid metals. To prevent backstreaming of the reactant gas, a hydrogen push gas inlet was built in at the upstream end of the growth vessel.

B. Growth of InP Using Cylinder HCl

1. Experimental Procedure

Six 9's pure indium was etched in a 45% KOH solution for about 30 min., and then baked in prepurified hydrogen [15]. The furnace controllers were then set to provide a flat 800°C region for the source zone and a

flat 650°C region for the deposition zone, and then a polished and cleaned [15] (001) semi-insulating iron doped substrate was placed in the forechamber. The chamber was pumped down and backfilled with hydrogen several times, and then the gate valve was opened and the substrate was magnetically inserted into the predeposition zone. The deposition gases were diverted from the substrate while it was being heated up in a phosphine stream, and then the substrate was moved into the deposition position. The flow rate of the HCl and PH_3 are varied, but the total flow rate was fixed at 500 ccm. A film was grown for thirty minutes, the substrate was retracted into the forechamber closing the gate valve behind it, and the deposition gases were turned off. A downstream HCl gas flow was turned on to clean out the growth tube. The forechamber is pumped down and back filled several times, and then the film is removed.

First, the morphology is examined and then photographed using an optical microscope. Contacts are put on in a van der Pauw geometry, and the room temperature and liquid nitrogen carrier concentrations and mobilities were measured. A portion of the substrate was cleaned off, etched in on AB etch for 5 min. at 60°C, [16] and then the film thickness was measured using the optical microscope. The remaining substrate was examined and photographed in a SEM.

Next, optical and scanning electron micrographs were taken of the surfaces. Both the gross structure and details of the fine structure were examined.

2. Results

a. Morphology

The effects of varying the input HCl concentration are illustrated in the optical micrographs in figures 1 and 2. The HCl/PH_3 ratios are

.25/1.5, .5/1.5, 1.0/1.5, 1.5/1.5, 3.0/1.5, and 4.0/1.5 in figures 1a, 1b, 1c, 2a, 2b, and 2c respectively. (To obtain the partial pressure of each species multiply by 10^{-2} atm.). The film with the smallest ratio is somewhat rough and contains star like characters with a pit in the center. The films with the .5/1.5 and 1.0/1.5 ratios are, for the most part, smooth. An enlargement (300x) of one of the few defects in the 1.0/1.5 film is displayed in figure 1d. The films with the larger ratios are rough as they contain many hillocks, and the roughness increases with the ratio.

The fine structure of some of these morphological defects are shown in the scanning electron micrographs in figure 3. In figure 3a the center of the needle shaped facets in figure 2a are square spirals surrounding a defect which is possibly an indium droplet. A top of a pyramid shown in figure 2c is magnified in figure 3b. It appears as if a number of grains have grown together around a rectangular defect. The white spots are most likely contaminants dropped onto the film while preparing the sample for the SEM.

The effects of varying the PH_3 pressure are illustrated in figure 1c and 4 for films with the ratios 1.0/1.5, 1.0/2.0 and .5/6.0. The 1.0/1.5 film is smooth, the 1.0/2.0 film contains oval morphological defects, and the .5/6.0 film has a gross arrowhead structure.

The fine structure of the oval morphological defect in figure 4b is shown in the scanning electron micrograph in figure 5. There it is seen that these defects are pits.

The effects of varying both the HCl and PH_3 concentrations while keeping their ratio constant is illustrated in figures 4a and 6. The .25/.50 film is smooth, the .5/1.0 film contains bunched pyramids, and the 1.0/2.0 film has oval morphological defects.

(a)

(b)

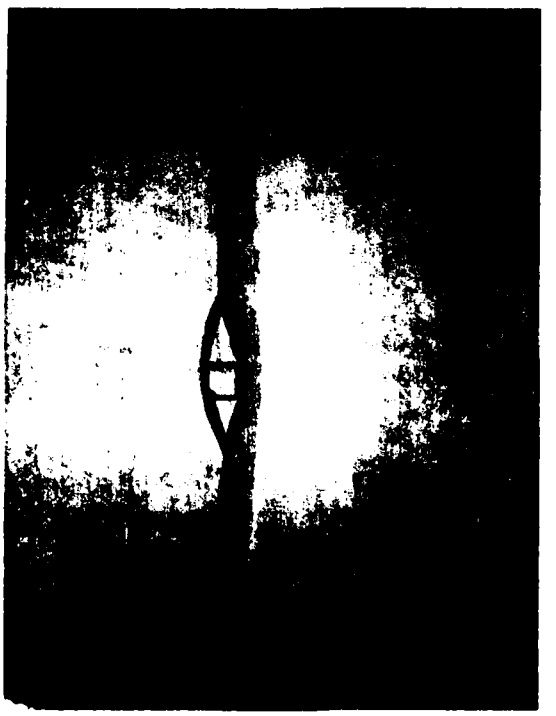

(c)

(d)

Fig. 1. Photomicrographs of films grown with III/V ratios of a.) .25/1.5 (37.5x), b.) .5/1.5 (37.5x), c.) 1.0/1.5 (37.5x), and d.)1.0/1.5 (300x).

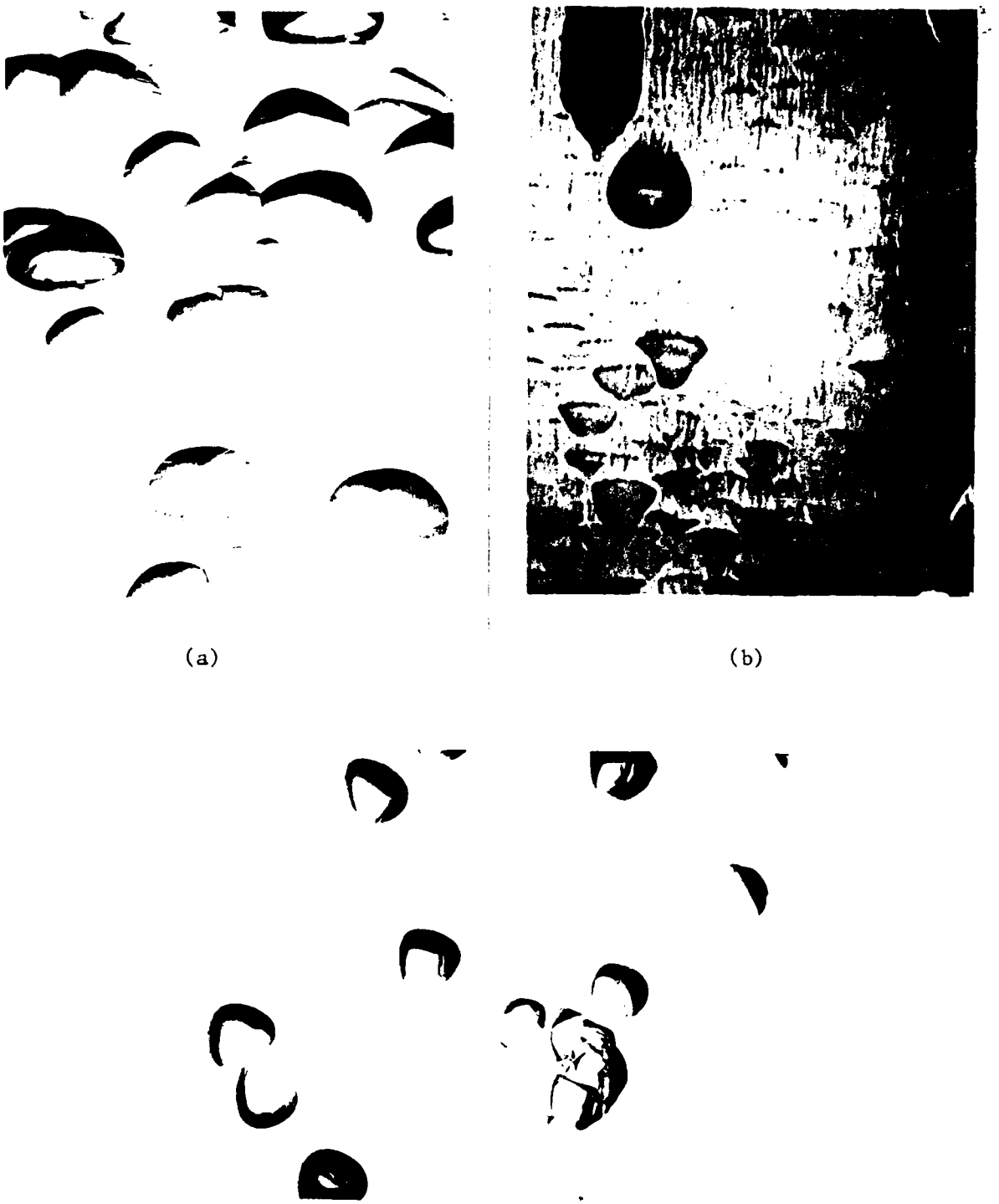

(a) (b)

(c)

Fig. 2. Photomicrographs of films grown with III/V ratios of a.) 1.5/1.5 (37.5x), b.) 3.0/1.5 (37.5x), and c.) 4.0/1.5 (37.5x).

(a)

(b)

Fig. 3. Scanning electron micrographs of films grown with III/V ratios of a.) .25/1.5 (215x) and b.) 4.0/1.5 (360x).

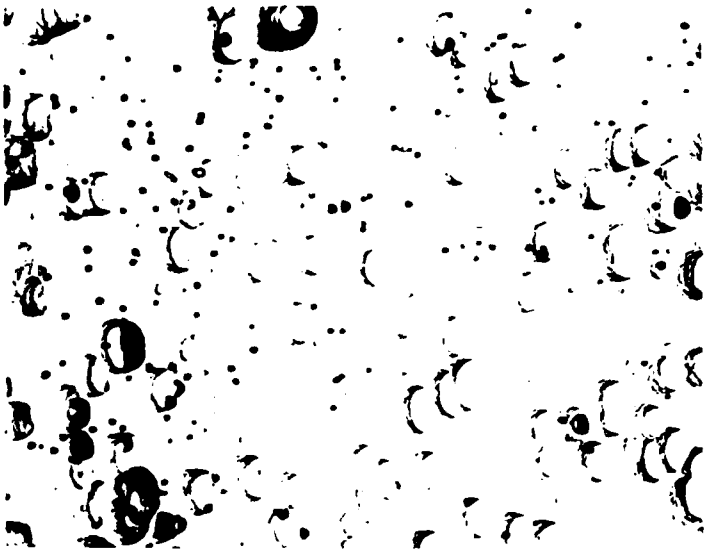

(a)

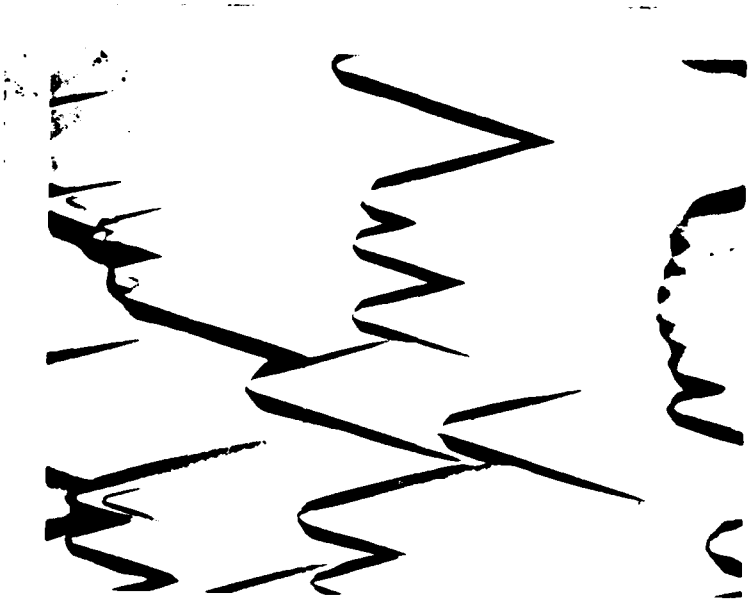

(b)

Fig. 4. Photomicrographs of films grown with III/V ratios of a.) 1.0/2.0 (37.5x), and b.) .5/6 (37.5x).

Fig. 5. Scanning electron micrograph of a film grown with III/V ratio of 1.0/2.0 (575x).

(a)

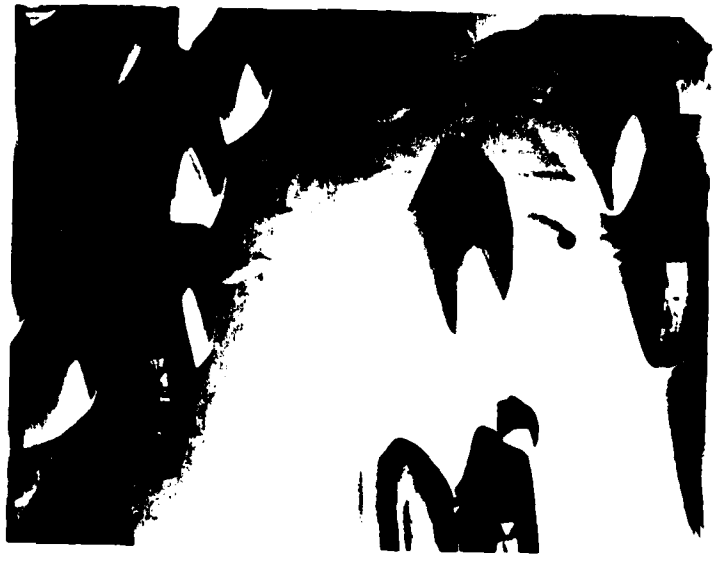

(b)

Fig. 6. Photomicrographs of films grown with III/V ratios of a.) .25/.50 (37.5x), b.) .5/1.0 (37.5x).

The fine structure of the oval morphological defects was previously illustrated in figure 5. The fine structure of the bunched pyramids is displayed in figure 7.

Micrographs of films deposited at 600, 650, and 700°C are displayed in figures 6a and 8. The low temperature film is very rough, the middle temperature film is smooth (fig. 6a), and the high temperature film is grainy. The fine structure of the high temperature film is shown in the scanning electron micrographs in figure 9.

b. Carrier Concentration and Mobility

The room temperature and liquid nitrogen carrier concentrations and mobilities are listed in table 1 along with the average growth rate.

3. Discussion

a. Morphology and Growth Rate

Smooth films can be grown at 650° when the III/V ratio is .5-1.0/1.5. This is similar to the results obtained by Zinkiewicz et al [6]. At higher HCl flow rates pyramids appear on the surface and at higher PH_3 flow rates pits appear. This is also similar to the results of Zinkiewiez et al, [6] and the results of Enstrom et al on GaAs [9].

For the chloride process, however, smooth films can be grown at PCl_3 pressures of .02 atm. [7,8,17-19]. The equivalent III/V ratio for this pressure is 6.0/2.0. One can speculate that the HCl pressures must be lower in the hydride system because in this system the HCl more effectively reacts with the liquid indium. It is also possible that the higher indium arrival rate due to the larger flow rate in the hydride system does not allow the indium sufficient time to surface diffuse to its equilibrium position. An alternative, but less likely possibility, is that the InCl does not as effectively react with the PH_3. There is more PH_3 present in the hydride system because it does not very quickly dissociate [20,21].

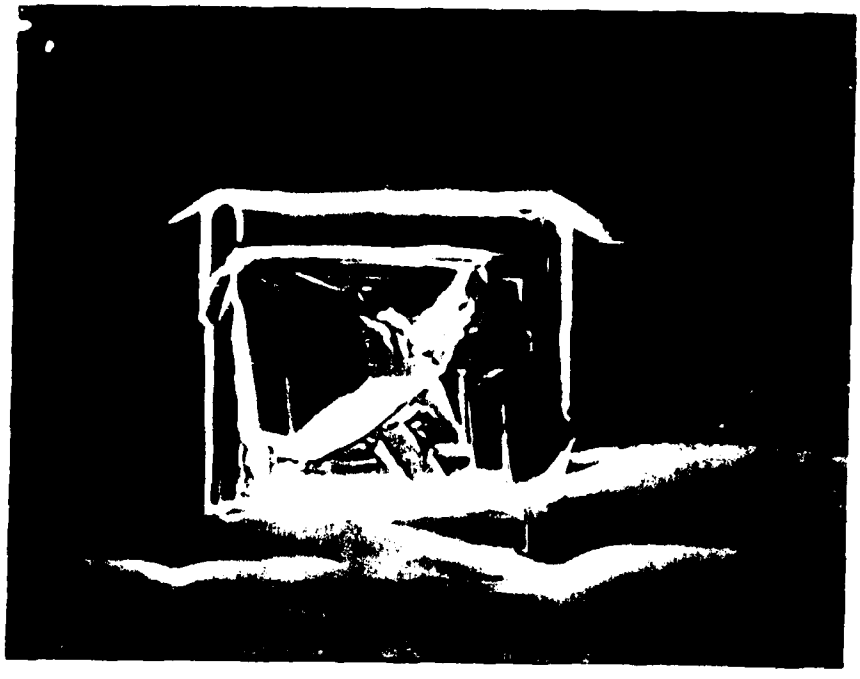

Fig. 7. A scanning electron micrograph of a film grown with a III/V ratio of .5/1.0.

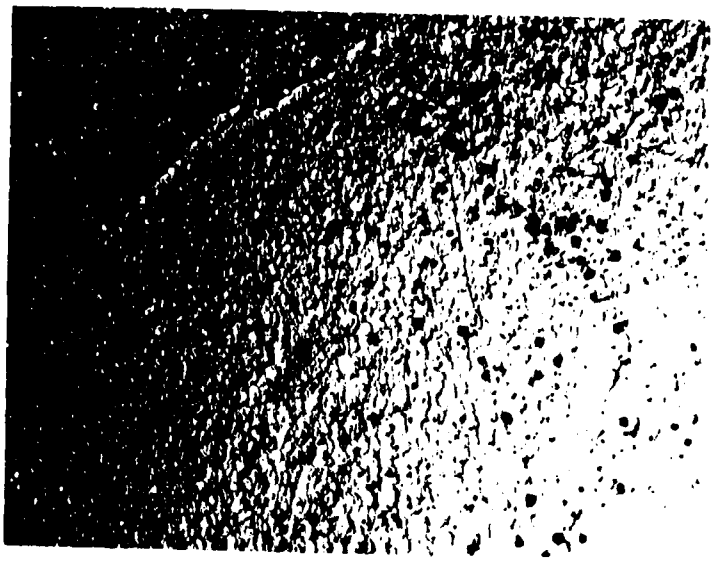

(a)

(b)

Fig. 8. Photomicrographs of films grown with III/V ratios of .25/.50 at a.) 600 (37.5x), and b.) 700°C (37.5x).

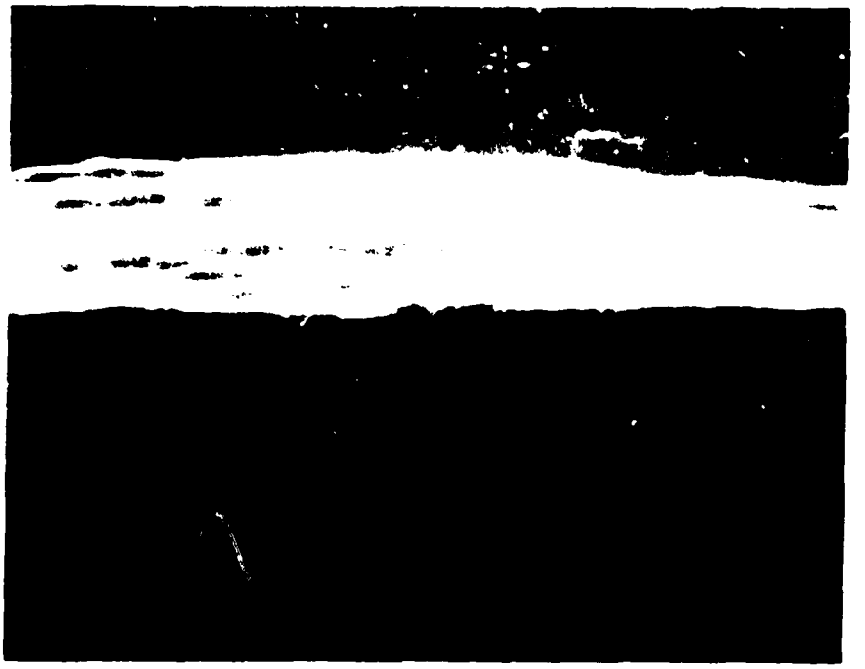

Fig. 9. A scanning electron micrograph of a film grown with a III/V ratio of .25/.50 at 700°C.

TABLE 1

The room temperature and liquid nitrogen carrier concentrations and mobilities and the growth rate of some InP films.

Sample No.	HCL^{o}/PH_3^2 Ratio	n(RT) cm^{-3}	n(LN) cm^{-3}	μ(RT) $cm^2/V.sec$	μ(LN) $cm^2/V.sec$	Growth Rate microns/min
25	.5/1.5	$2.2x10^{17}$	$5.51x10^{16}$	2700	4020	.09
33	1.0/1.5	$4.92x10^{16}$	$1.11x10^{16}$	666	2100	.32
38	1.5/1.5	$6.84x10^{17}$	$7.00x10^{17}$	772	705	1.17
35	3.0/1.5	$5.48x10^{18}$	$5.86x10^{18}$	543	461	.22
36	4.0/1.5	$1.03x10^{18}$	$1.09x10^{18}$	478	517	1.00
32	.25/.50	$1.30x10^{17}$	$5.53x10^{16}$	532	1370	.25
31	.25/1.5	$3.65x10^{16}$	$1.11x10^{16}$	602	2300	.30
27	.25/3.0	$3.27x10^{16}$		1200		.39
28	.25/4.5	$3.29x10^{16}$	$1.32x10^{16}$	305	820	.11

This explanation is less likely because it is generally thought that PH_3 reacts more, not less, effectively with InCl than does P_2 or P_4 [6-8,17-19]. For example, PH_3 and InCl could form an adduct, and then the hydrogen and chlorine atoms could be removed by a simple elimination reaction.

As one would expect, the film morphology changes when the substrate temperatuare changes even if the flow conditions remain constant. Also, the III/V ratio for smooth films is different when the III and V pressures change.

The growth rate increases substantially with the HCl concentration and only gradually with the PH_3 concentration. This has been observed by Shaw [22] and Enstrom [9] et al for GaAs, and it is what one would expect from thermodynamics [23]. This is due to the fact that the supersaturation changes more rapidly with the HCl concentration than with the PH_3 concentration.

b. Carrier Concentration and Mobility

Even though the InP films were only grown to test the 'upgraded' system, and there was no attempt to optimize the film properties, the carrier concentrations were much higher and the mobilities were much lower than they were in our earlier tests. Our admittedly speculative explanation is that in 'upgrading' our system we increased the InCl concentration too much by increasing the contact between the HCl and the liquid indium by using a covered boat, and increasing the residency time of the HCl over the indium by decreasing the flow rate. This explanation is, at least, consistent with the observation that the carrier concentration increased with the HCl concentration, but did not increase with the PH_3 concentration.

Other possible explanations are that the furnace often was not kept hot between runs, the system contains substantial leaks, the gases used

were impure, or there was out diffusion from the substrate. Not keeping the furnace continuously on could result in contamination from material that had deposited on the side walls during cool down after the previous run. This is not a likely explanation because there appears to be no difference between the films that were grown consecutively, and those that were run between cool down interruptions. It does not seem likely there were any substantial leaks because the system was periodically leak checked down to 10^{-9} atm. cc/min. The gases used were LED purity gases from Matheson. The HCl purity could have decreased with time as it could have slowly reacted with the cylinder. Although a little iron might out diffuse from the substrate, it does not seem at all likely that the concentraton in the film could be large enough to account for the observed behavior.

c. Growth of InP Using HCl from PCl_3

The cracking furnace illustrated in figure 10 was installed. The highlights are that HCl can be generated from the ultrapure trichlorides, $AsCl_3$ or PCl_3, [24] for purposes of comparison films can be grown directly using the chloride method, and the system is an all quartz system eliminating any possibility that the HCl will react with stainless steel.

The system works as follows. Hydrogen is bubbled through the trichloride and then flows through the cracking furnace. If the single zone furnace is turned on to its operating temperature of 900°C, the trichloride - H_2 mixture decomposes into HCl and primarily into the tetramer and lesser amounts of the dimer and the trihydride [23,25]. The dimer and the tetramer precipitate out in the cold trap and the HCl and a small amount of the trihydride flow to an inlet that leads to one of the cation boats. If the results for this system are promising, the output HCl from the cracking system will be directed to two flow meters

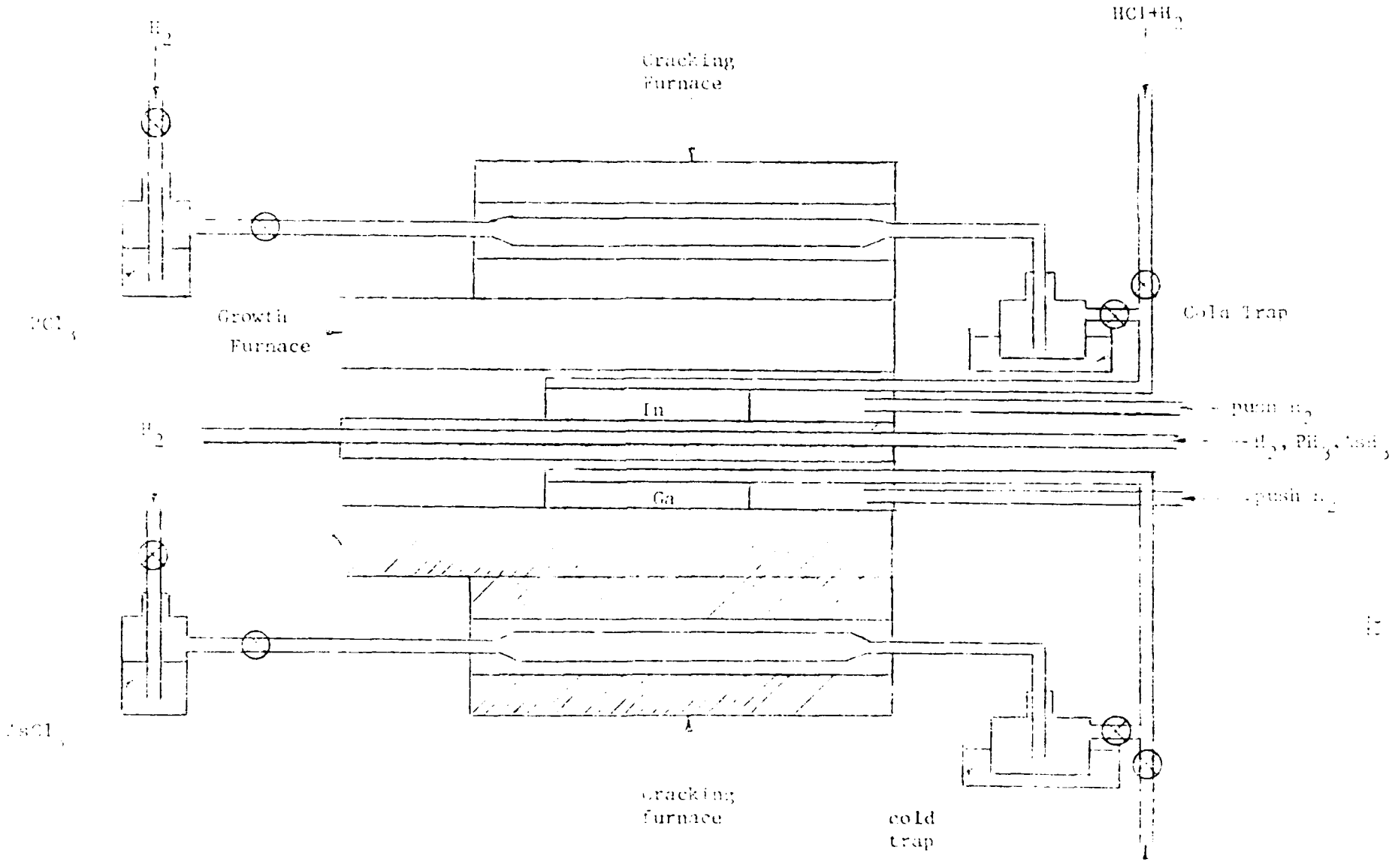

Figure 10. Schematic of the cracking furnace for the anion chlorides.

set up in parallel so that the HCl flow to each cation boat can be separately controlled.

If the cracking furnace is not turned on, the trichloride will flow directly to the cation boat. In this way a binary film can be grown directly using the chloride method. This should prove to be useful in trying to understand why chloride films can be grown with a smaller background carrier concentration than hydride grown films.

Recently, we grew InP films using HCl generated by decomposing PCl_3 in hydrogen in a cracking furnace at 900°C. We report here our initial findings and will describe our results in more detail in the next quarterly report.

The InP films grown using this HCl was much better. The carrier concentrations were in the low 10^{16} and high 10^{15} cm^{-3}, the room temperature mobilities were 3000 $cm^2/V \cdot sec$ and the liquid nitrogen mobilities were 20,000 $cm^2/V \cdot sec$. We, therefore, conclude that our poor previous results were due to contaminated HCl. The HCl had been in the cylinder for more than one year so it could have degraded by reacting with the cylinder. This conclusion is made more plausible by the fact that the films we grew when the bottled HCl was fresh were better films.

These recent results still are not as good as those of Zinkiewicz et al [6], but they are close. We are optimistic that we will soon be able to match them.

C. Growth of InGaAs Films

The InP substrate was polished and cleaned in the same way it was for the growth of an InP film, and it was also mounted and inserted into the preheat zone in the same manner. For the preheat treatment the substrate was bathed in either .5% PH_3 or .5% AsH_3 in purified hydrogen for a period

of five minutes. The total flow rate of 500 ccm included an HCl flow rate of 3 ccm over the gallium, an HCl flow rate of 18-30 ccm over the indium, and an AsH_3 flow rate of 12 ccm. Thus, the HCl(In)/HCl(Ga) ratio varied from 6:1 to 10:1 and the III/V ratio varied from 1.75:1 to 2.75:1. The source temperature was 800°C, the deposition temperature was 700°C, and the growth time was 70-80 minutes.

The films were quite smooth. A representative morphology is illustrated in figure 11. As can be seen in the higher magnification scanning electron micrograph (2140x), the morphological defects are truncated square pyramids. The base of the pyramid is rectangular instead of square due to the fact that the sides of pyramid have alternating A and B orientations.

There were no general trends in the morphologies as the HCl(In)/HCl(Ga) and the III/V ratios were varied. However, it did appear that the film was smoother when the substrate was preheated in AsH_3 than when it was preheated in PH_3. For one run, the substrate was also etched with .05% downstream HCl, and this film appeared to have the best morphology. We will investigate this further during the next quarter.

Films grown on substrates bathed in AsH_3 also had smaller rocking curve widths. This is shown in the (400) rocking curves in figure 12. The curve was found using a Lang camera with a fine focus tube and a beam extender. The peak width at half maximum for the PH_3 preheated sample was 1830 secs. whereas it was 1225 secs. for the AsH_3 preheated specimen. For the single run we did using a downstream HCl etch, we found that the peak width was even smaller - 700 secs. We plan to investigate the effects of the downstream HCl in more detail. For all of these specimens the lattice mismatch was greater than 1%. Thus some of the peak breadth is due to the mismatch strain. Also, our system is not as precise

Figure 11. Morphology of an InGaAs Film. a.) 214X and b.) 2140X.

as a double crystal measurement. The peak breadth attributable to the less precise measuring device can be determined from the rocking curves for the InP substrate illustrated in figure 12b. There it is seen that the K_{α_1} and K_{α_2} peak breadths are 270 sec. This compares to a value of 25 secs for a double crystal system.

From the rocking curve in figure 12c we can show that the lattice mismatch was .5% for the In/Ga ratio of 7:1. This mismatch was substantially smaller than it was for the other films.

Yamauchi et al [26] also have found that the surface preheat treatment has a pronounced effect on the rocking curve width. They found that with a cover piece the peak width, as determined with a double crystal monochromator, was 25" for lattice matched InGaAs whereas it was as large as 500" for lattice matched InGaAs when no cover piece was used. At the same growth temperature and HCl(Ga) partial pressure Hyder et al [27] obtained lattice matching for an In/Ga ratio of 10.5 and a III/V ratio of 3:1 whereas Kanbe et al [28] obtained lattice matching for an In/Ga ratio of 2.1:1 and an undetermined III/V ratio.

The room temperature mobilities and carrier concentrations determined using a Hall effect device are shown in table 2. Measurements were not made at liquid nitrogen temperatures since the films were not lattice matched.

Our mobillties, while encouraging, are not as high as those achieved by others [28-33]. The highest reported value for hydride grown films is 10,050 which was achieved by Kanbe et al. [28]. We believe that we will be able to improve our results by replacing flow meters with flow controllers so that we can more reproducibly obtain lattice matching, generating HCl by cracking $AsCl_3$ which should be more pure than the HCl

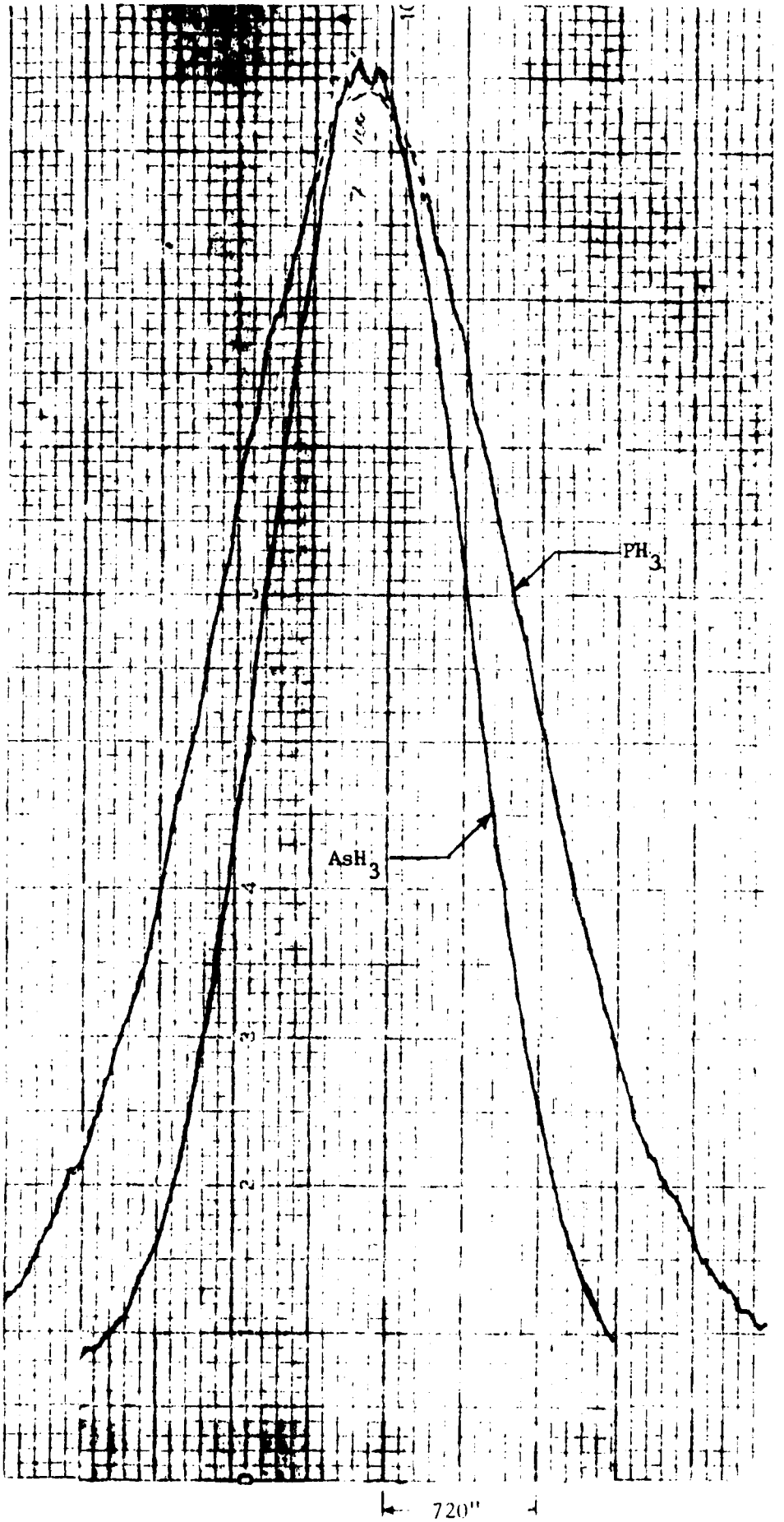

Fig. 12a. Rocking curves for InGaAs films grown on InP substrates preheated in PH_3 or AsH_3.

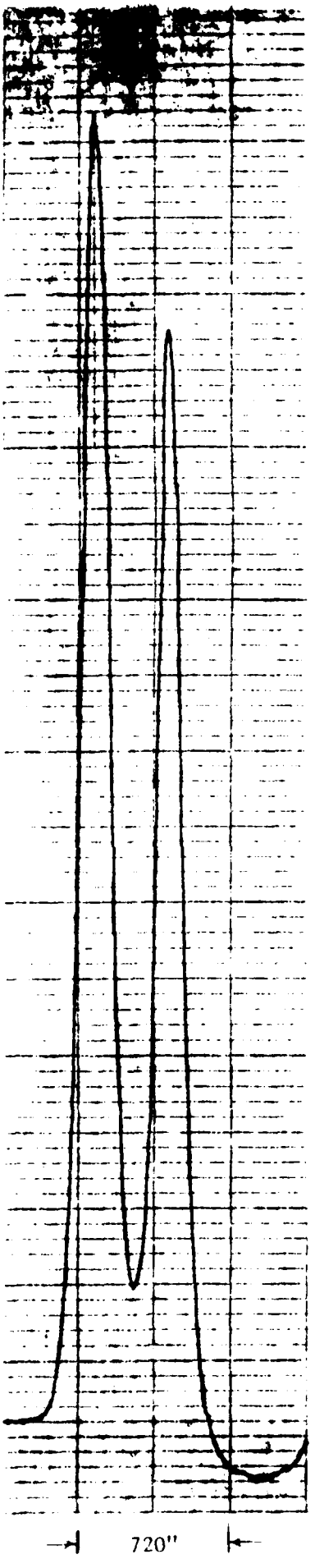

(b)

Fig. 12b. K_{α_1} and K_{α_2} peaks for an InP substrate

Fig. 12c. Rocking curve for an InGaAs film lattice matched to within .5% of the InP substrate.

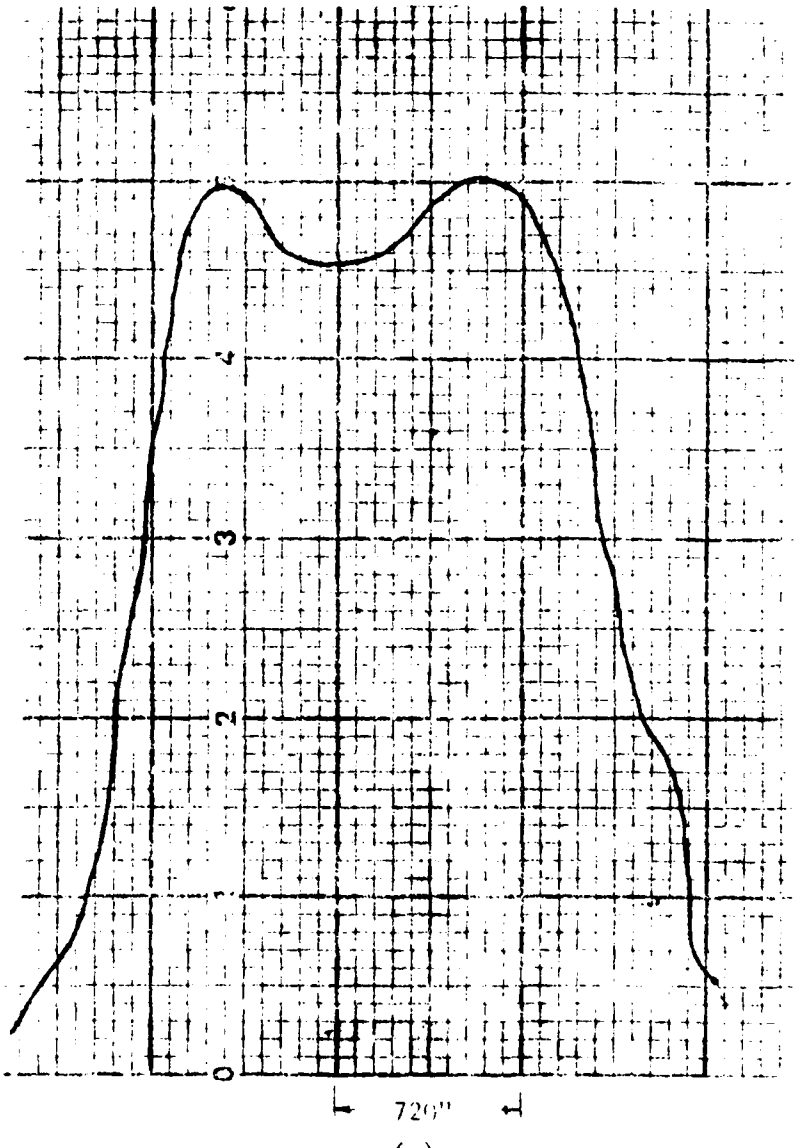

(c)

TABLE 2

The room temperature mobility and carrier concentration and growth rate for InGaAs films grown under a variety of In/Ga and III/V ratios.

Specimen	In/Ga	III/V	$cm^2/V \cdot sec$	$n_d - n_a$ cm^{-3}	growth rate μ/hr.
82	$\frac{28.5}{3}$ = 9.5:1	$\frac{28.5}{12}$ = 2.3:1	3464	5.3×10^{16}	8.9
83	$\frac{22.5}{3}$ = 7.5:1	$\frac{22.5}{12}$ = 1.9:1	3436	6.2×10^{16}	11.2
84	$\frac{18}{3}$ = 6:1	$\frac{18}{12}$ = 1.5:1	3415	7.1×10^{16}	7.5
85	$\frac{21}{3}$ = 7:1	$\frac{21}{12}$ = 1.75:1	4510	4.1×10^{16}	13.1
86	$\frac{25.5}{3}$ = 8.5:1	$\frac{25.5}{12}$ = 2.1:1	3462	5.3×10^{16}	7.9
90	$\frac{24}{3}$ = 8:1	$\frac{24}{12}$ = 2:1	3434	5.7×10^{16}	9.2

obtained from a gas cylinder, and using a downstream HCl etch to improve the quality of the InGaAs/InP interface.

The background carrier concentrations were higher than those obtained by others [29-33]. Again, we are confident that we will be able to improve on these values if we generate HCl from ultrahigh purity $AsCl_3$, and if we use a downstream HCl etch during the preheat treatment.

Our growth rates are about half those observed by Hyder et al. [27]. With similar partial pressures and a growth temperature of 688°C they measured a growth rate of 21.6 μ/hr. However, their flow rates were twice as large as ours which accounts for the factor of two in the mass transport limited regime.

D. Surface Studies

1. Experimental Procedure

For the surface studies the substrates were handled in the same manner. Except for the sample which was covered with a cover piece in

the MO-CVD system, the other samples were inserted into the deposition zone where they were unbathed or bathed in PH_3, AsH_3 or HCl. Different exposure times and temperatures were used.

After the sample was removed from the forechamber, it was placed in a desicator with P_2O_5 in an attempt to reduce surface contamination from the atmosphere. Immediately after the last sample was prepared, the samples were transported to the ESCA apparatus and loaded into the system. The sample holder is a stainless steel jig with molydenum masks. The -ray source is a 600 watt aluminum anode, the analyzer is a double pass cylindrical mirror analyzer, and the sputtering beam etching source is an argon ion source with a broad power range.

2. Results

Optical micrographs of a substrate exposed only to hydrogen gas at 650°C for thirty minutes, and a substrate partially covered by a tantalum foil and bathed in 1.5% PH_3 are shown in figure 13. The substrate exposed only to hydrogen shows the characteristic rectangular pits created by phosphorus evaporation. The photograph of the partially covered film indicates that there is possibly some phosphorus deposited on the surface.

The fine structure of the rectangular pits is shown in the scanning electron micrograph in figure 14. There it is seen that the small slits in figure 13 are also rectangular pits.

The qualitative results of an ESCA examination of substrates subjected to different heat treatments in our InGaAs growth vessel are listed in table 3. The treatments include exposing the substrate surface at 650°C for 15 min. to H_2 only, H_2 - 1.5% PH_3, H_2 - 1.5% AsH_3, and H_2 - 1.5% HCl mixtures, as well as being covered by a cover piece.

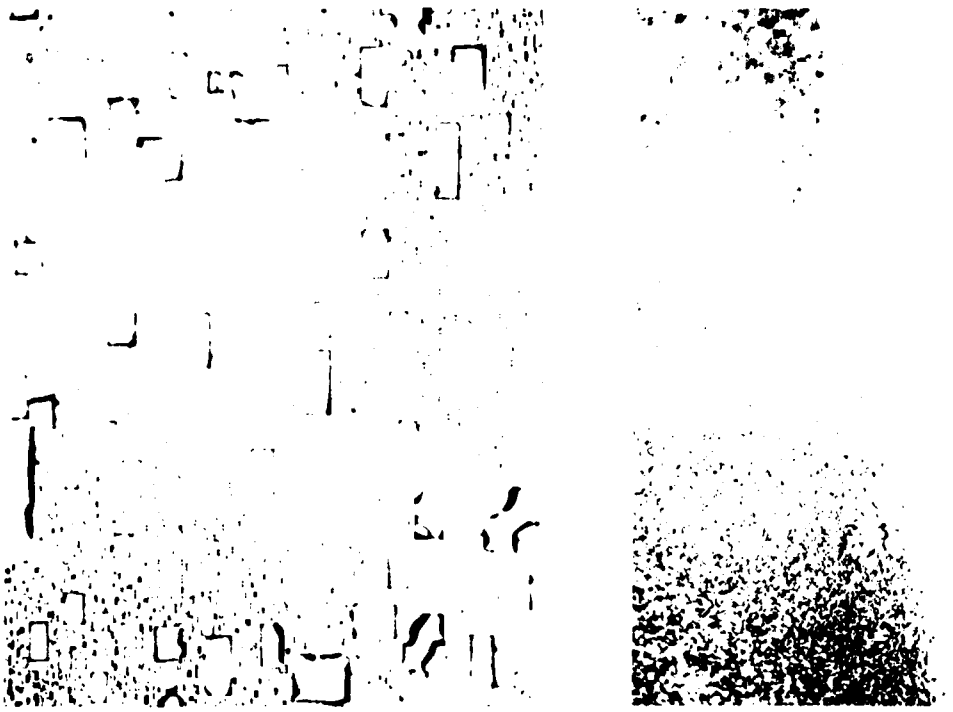

Fig. 13. Photomicrographs of a.) a substrate exposed to H_2 only for 30 min. at 650°C (37.5x) and b.) a partially covered substrate bathed in PH_3 at $1.5x10^{-2}$ atm. for 30 min. at 650°C (37.5x).

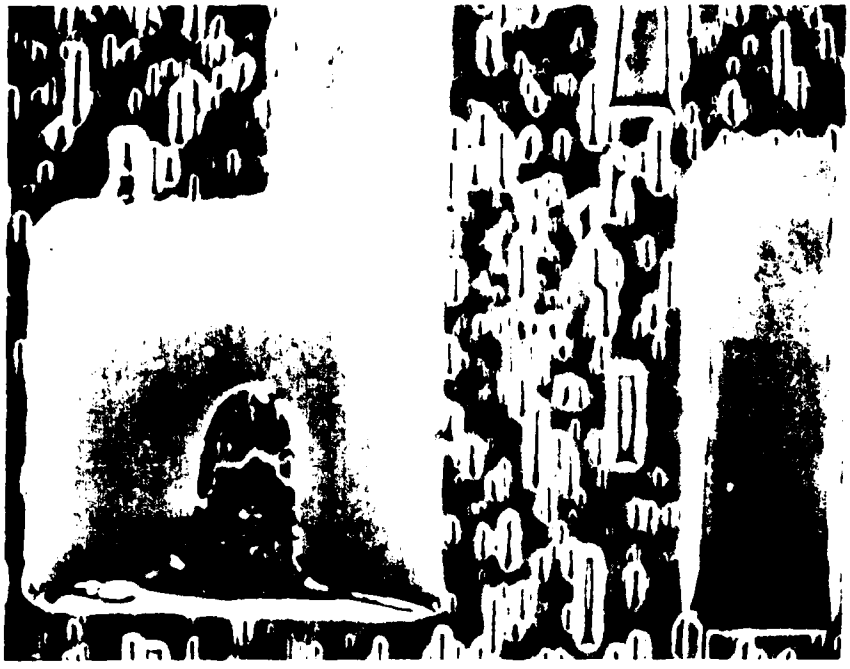

Fig. 14. A scanning electron micrograph of a substrate exposed to H_2 for 30 min. at 650°C (1440x).

TABLE 3

The qualitative results of an ESCA analysis of the surface of a substrate subjected to different environments at 650°C for 15 minutes.

Heat Treating Gas	Observations
1. H_2	a. P concentration down a little b. Substantial amount of As c. Substantial amount of Ga
2. PH_3	a. P concentration unchanged b. A small amount of Ga c. No As
3. AsH_3	a. P concentration down a little b. A large amount of As c. A small amount of Ga d. The largest oxygen concentration
4. HCl	a. P concentration unchanged b. No As c. No Ga
5. Cover Piece	a. P concentration unchanged b. A small amount of As c. A small amount of Ga

3. Discussion

The surface of the substrate heated in H_2 only for 30 min. is similar to the surface observed by Clawson [34,35] et al. when it was subjected to a similar heat treatment. The rectangular shape of the pits is due to the uneven etch rates of the <111> A and B facets. The surface exposed to a .01 atm. flow of PH_3 contains small surface defects. It is likely that this is phosphorus deposited from the vapor as the pressure is substantially above the phosphorus pressure in equilibrium with the InP [35]. The smoothest surface is the surface covered by a cover piece. Apparently the phosphorus pressure under the cover piece is large enough to prevent appreciable phosphorus evaporation.

Some of the results of the surface analysis are what one would expect. The phosphorus concentration is reduced in the substrates exposed to H_2 and the AsH_3 mixture, the surface exposed to the AsH_3 mixture contains a substantial amount of arsenic, gallium and arsenic from the growth vessel contaminate the substrate surface, and there was no discernible loss of phosphorus from the substrate exposed to the PH_3 mixture or the substrate covered by the cover piece. Some results that could not be so readily predicted are that the HCl surface was the cleanest and the AsH_3 surface contained the most oxygen. We were initially surprised that the covered substrate contained gallium and arsenic, but we later realized that the cavity had been contaminated during previous growth runs.

4. Effects of Downstream HCl Etch

Recently, we determined that we could grow smoother films if we etched the substrate with a dilute ($\sim 10^{-3}$ atm.) downstream HCl much like Ghandhi [36-37] and his coworkers have done. This subject will be discussed

in greater detail in the next quarterly report. Not only do we expect that the downstream etch will improve the quality of InP films, we expect it to also improve the quality of the InGaAs films.

III. Theoretical Studies

A. Hydride and Chloride Comparison

1. Physical Analysis

There are a number of similarities between the growth of InP films using the hydride [6] and chloride [7-8,17-19] techniques. In both instances indium is transported by the monochloride; phosphorus is present as P_4, P_2 and PH_3; the growth rates initially increase with the InCl concentration; and the deposition reactions are identical. The primary differences are that the reactions in the source zone are different; the cation and anion concentrations are separately controlled in the hydride process; and the phosphorus containing compounds are introduced into the deposition zone via different routes.

In the hydride process the only significant reaction in the source zone is the reaction between liquid indium and HCl leading to the formation of InCl. There are, however, a number of simultaneous reactions in the chloride system. First, the PCl_3-H_2 mixture completely decomposes to HCl, P_4, P_2 and PH_3. The phosphorus containing compounds react with the liquid indium to form an InP film, which is attacked by one third of the HCl - the other two thirds attacks the indium. At some time a steady state is reached when the rate of formation of the InP film is the same as the rate of attack by the HCl. (It is this transient time that makes it difficult to grow multilayered structures with abrupt junctions using the chloride process).

The phosphorus in the hydride technique is introduced by injecting PH_3 downstream, whereas in the chloride system P_4, P_2 and PH_3 are

PCl_3-H_2 decomposition products or reaction products of the HCl-InP reaction. The P_4, P_2 and PH_3 introduced into the deposition zone are, therefore, more likely to be in thermodynamic equilibrium in the chloride system. This is particularly true for PH_3 because it decomposes rather slowly [20,21].

In this discussion the source zone equilibrium vapor composition in the hydride system, and the steady state vapor composition in the chloride system are computed for different input HCl or PCl_3 compositions. The deposition zone equilibrium vapor compositions are also calculated for different input HCl or PCl_3, downstream HCl or PCl_3, and input PH_3 pressures. Of particular interest are the deposition zone HCl partial pressure since it is thought that HCl controls the degree of silicon contamination, and the supersaturation because it determines the ideal growth rate. The computed trends of the HCl pressure are compared with the trends of the background carrier concentration, and the computed trends of the ideal growth rate are compared with the experimentally determined growth rates to see if they can be explained thermodynamically.

In the computations that follow it will be assumed that the temperatures chosen - 750°C for the source zone and 650° for the deposition zone - are high enough and the gas flow rates are low enough for growth to be in the thermodynamically limited mass transport regime. Also, in the graphs and tables the PCl_3 pressures will be compared with HCl/3 pressures since upon the decomposition of PCl_3, three units of HCl are formed. Comparisons will be made for 'normal' growth conditions for which the input HCl pressure is .03 atm. and the input PH_3 and PCl_3 pressures are .01 atm., and for pressures one third and three times these values.

In the hydride source zone HCl reacts with liquid indium according to the equation,

$$3HCl + 3In(\ell) \rightarrow 3InCl + \frac{3}{2} H_2 \qquad (1a)$$

This assumes that $InCl_3$ does not form; there is theoretical evidence that this is the case [25].

There are a series of simultaneous source reactions in the chloride system. Taken separately they are: the thermal decomposition of PCl_3, the HCl-liquid indium reaction, the reaction of the phosphorus containing compounds with liquid indium to form InP, and the HCl attack of InP. (see Fig. 15).

The PCl_3 decomposition reaction is

$$PCl_3 + \frac{3}{2}(1+y)H_2 \rightarrow (1-y)\frac{x}{2} P_2 + (1-y)(\frac{1-x}{4})P_4 + yPH_3 + 3HCl \qquad (2)$$

and is essentially complete. At 750°C the equilibrium $P_{PCl_3} = 2.15 \times 10^{-11}$, $P_{P_4} = 2.34 \times 10^{-3}$, $P_{P_2} = 7.05 \times 10^{-4}$, $P_{PH_3} = 2.86 \times 10^{-4}$, and $P_{HCl} = .03$ atm. when .01 atm. of PCl_3 is mixed with one atm. of hydrogen [23].

Because the HCl can attack both the liquid indium and the InP, equation 1a for the reaction with liquid indium must be modified to

$$(3-z)HCl + (3-z)In(\ell) \rightarrow (3-z)InCl + \frac{1}{2}(3-z)H_2 \qquad (1b)$$

In the beginning when there is no InP to attack, $z = 0$.

For illustrative purposes it is assumed that the HCl comes into equilibrium with the liquid indium, and then the phosphorus containing

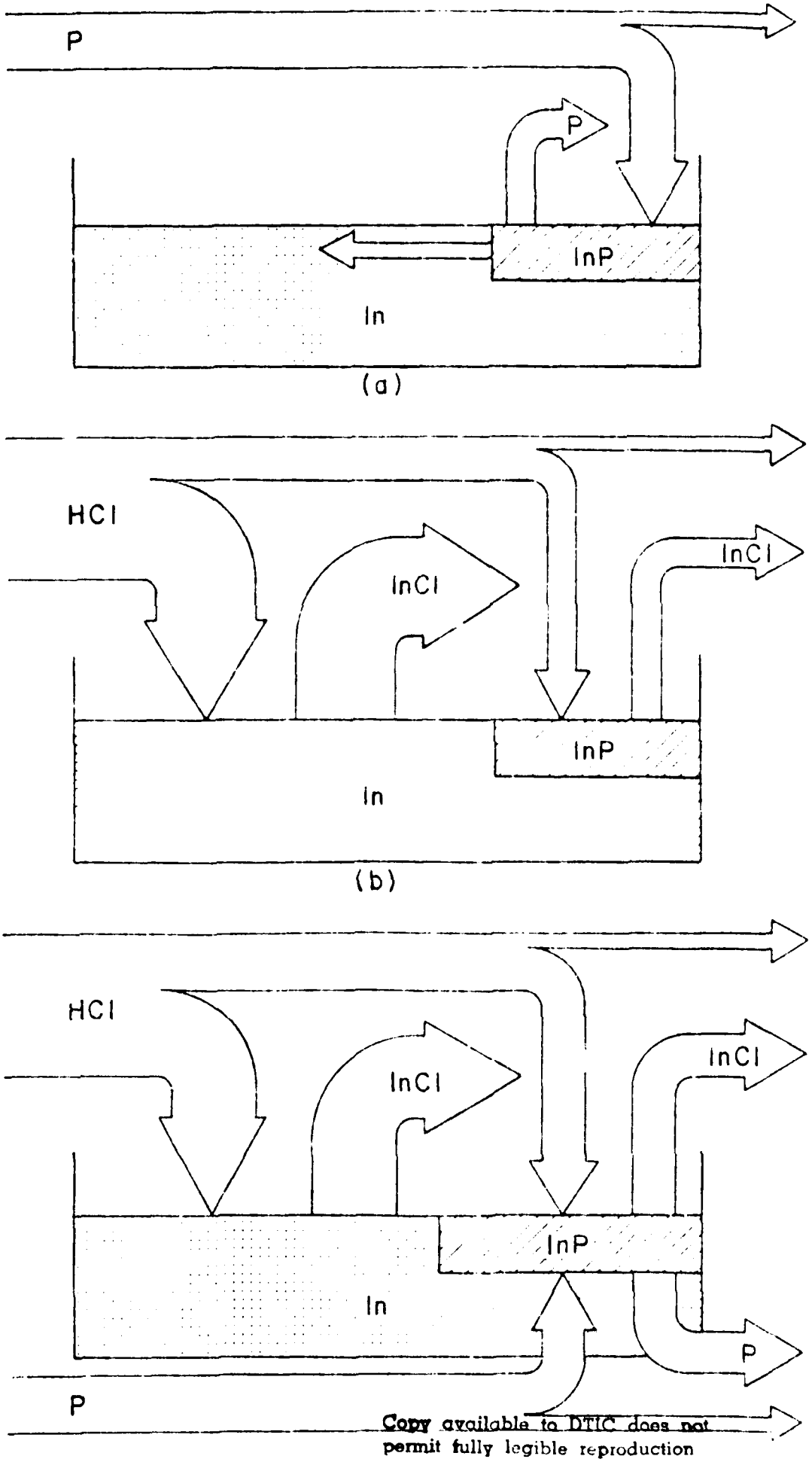

Fig. 15. The transient behavior of the formation of the InP crust in the chloride system. a.) More phosphorus is reacting wi
the liquid indium than is being generated by the attack of InP by HCl; b.) more than 2/3 of the HCl is reacting with
the liquid indium, c.) the steady state condition when the same amount of phosphorus is being generated as is
reacting, and 2/3 of the HCl is reacting with the liquid indium and 1/3 of it is reacting with the InP.

Copy available to DTIC does not
permit fully legible reproduction

compounds react with the liquid indium according to the equation

$$In(\ell) + (1-y)\frac{x}{2}P_2 + (1-y)\frac{(1-x)}{4}P_4 + yPH_3 \rightarrow InP(s) + \frac{3}{2}yH_2 \qquad (3)$$

The InP is then attacked by the HCl according to

$$zInP(s) + zHCl \rightarrow zInCl + z(1-y)\frac{x}{2}P_2 + z(1-y)\frac{(1-x)}{4}P_4 + zyPH_3 + \frac{z}{2}(1-3y)H_2 \qquad (4)$$

As z increases from zero to one, the net rate of formation of InP decreases to zero. This can be seen by summing eqs. 1b, 3 and 4 to yield 1a. Thus, the steady state source chloride process is identical to the equilibrium source hydride process.

The deposition reaction for both techniques is the same. It is the reverse of reaction 4 for $z = 1$.

2. Mathematical Analysis

The designation of the input and output constituent pressures are illustrated schematically in Fig. 16. Those having a zero superscript are source zone input partial pressures, those having a one superscript are equilibrium source zone output pressures, those having a two superscript are downstream deposition zone input pressures, and those having no superscript are equilibrium deposition zone output pressures.

For the hydride source zone the chlorine balance is

$$P_{InCl}^{1} = P_{HCl}^{o} - P_{HCl}^{1} \qquad (5)$$

From the fact the total pressure is 1 atm.

$$P_{H_2} = 1 - P_{InCl}^{1} - P_{HCl}^{1} = 1 - P_{HCl}^{o} \qquad (6)$$

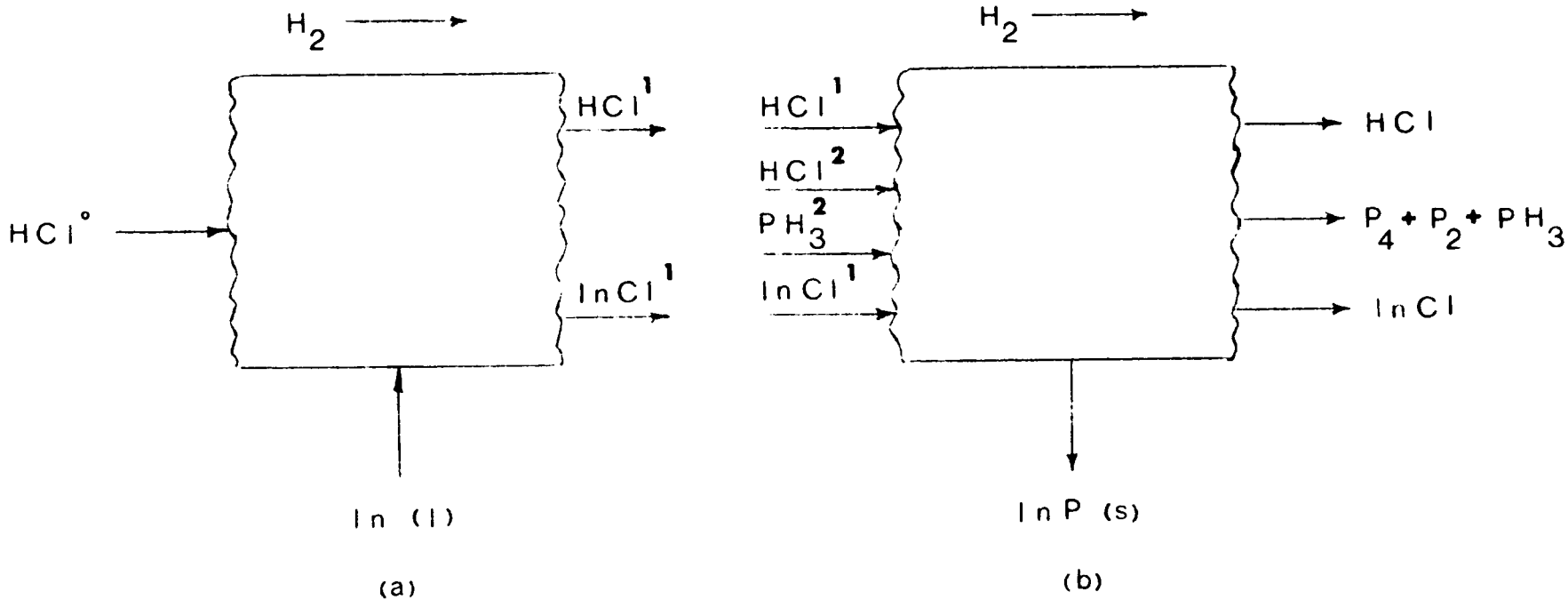

Fig. 16. The nomenclature used to designate the source (a) and deposition zone, (b) input and output constituents.

Then, P_{HCl^1} can be found from the equation

$$K_1 = \frac{P_{InCl^1} P_{H_2}^{1/2}}{P_{HCl^1}} = \frac{(P_{HCl^o} - P_{HCl^1})(1 - P_{HCl^o})^{1/2}}{P_{HCl^1}} \qquad (7)$$

with

$$RT\ln K_1 = - \Delta G_1$$

ΔG_1 can be found using the data tabulated by Shaw [25]. The fraction of HCl consumed by reaction 1, w, is

$$w = \frac{P_{InCl^1}}{P_{HCl^o}} \qquad (8)$$

The phosphorus and phosphine pressures in the chloride system before any InP is formed or after the steady state has been reached can be found in a straightforward manner. First, a value of P_{P_4} is assumed, and then it is used to compute P_{P_2} from

$$P_{P_2}^1 = P_{P_4}^{1\ 1/2} / K_{10}, \qquad (9)$$

where K_{10} is the equilibrium constant for the reaction

$$P_2 \rightarrow \frac{1}{2} P_4 \quad . \qquad (10)$$

P_{PH_3} is determined by the phosphorus balance

$$P_{PH_3^1} = P_{PCl_3^o} - 2P_{P_2^1} \quad 4P_{P_4}^1 \quad . \qquad (11)$$

The sum of the HCl and InCl pressures is constant so that

$$P_{HCl}^{1} + P_{InCl}^{1} = P_{HCl}^{o} = 3\,P_{PCl_3}^{o} \quad , \tag{12}$$

since all of the PCl_3 decomposes. The total pressure is 1 atm. so that

$$P_{H_2}^{1} = 1 - P_{P_2}^{1} - P_{P_4}^{1} - P_{PH_3}^{1} - 3P_{PCl_3}^{o} \tag{13}$$

The guessed value of P_{P_4} can now be checked by computing P_{PH_3} from the PH_3 dissociation reaction,

$$PH_3 \rightarrow \frac{x}{2} P_2 + \frac{(1-x)}{4} P_4 + \frac{3}{2} H_2 \tag{14}$$

and comparing it with the value obtained from eq. (11). The value of x^1 is found from

$$x^1 = P_{P_2}^{1}/(P_{P_2}^{1} + 2P_{P_4}^{1}) \tag{15}$$

and it is used to compute $P_{PH_3}^{1}$ from

$$P_{PH_3}^{1} = P^{x^1/2}_{P_2^1}\, P^{(1-x^1)/4}_{P_4^1}\, P^{1.5}_{P_{H_2}^1}/K_{14} \quad . \tag{16}$$

The pressures of the phosphorus containing molecules are at a minimum when they are in equilibrium with the liquid indium. This could occur at the beginning of the transient when the InP is just beginning to form and most of the HCl has been removed from the vapor by reaction with the liquid indium. Because they are transient pressures they are marked with an asterisk (*). Again the procedure begins by assuming a value of $P_{P_4^*}$, computing $P_{P_2^*}$ using eq. (9), and determining x^* with eq. 15. Because the phosphorus and phosphine pressures are so low,

$$P^{*}_{H_2} \simeq 1 - 3P^{o}_{PCl_3} \quad . \tag{17}$$

Now, $P^{*}_{PH_3}$ can be calculated using eq. (16), and it can be compared to $P^{*}_{PH_3}$ found from

$$P^{*}_{PH_3} = P^{*}_{H_2}/(P^{(1-y^{*})x^{*}/2}_{P_2^{*}} \; P^{(1-y^{*})(1-x^{*})/4}_{P_4^{*}} \; K_3)^{1/y^{*}} \tag{18}$$

after y^{*} has been determined from the equation

$$y^{*} = P^{*}_{PH_3}/(P^{*}_{PH_3} + x^{*}P^{*}_{P_2} + (1-x^{*})\,P^{*}_{P_4}) \tag{19}$$

The fraction, u, of the phosphorus consumed by the formation of InP is

$$u = (2P^{*}_{P_2} + 4P^{*}_{P_4} + P^{*}_{PH_3})/P^{o}_{PCl_3} \tag{20}$$

If the InP film completely covered the liquid indium - and it could only if more than two thirds of the HCl remained in the vapor or the film was partially composed of $InCl_3$ - the equilibrium partial pressures can be calculated from reaction (4). These partial pressures will be designed by a quotation mark ('). As before, a value for P'_{P_4} is assumed and P'_{P_2} and x' are calculated. P_{H_2} is given approximately by

$$P'_{H_2} \simeq 1 - P'_{P_2} - P'_{P_4} - 3PCl^{o}_{3} \; , \tag{21}$$

and P'_{PH_3} is found using eq. (16). This value of P'_{PH_3} is then compared with the value of P'_{PH_3} computed from the phosphorus balance,

$$P'_{PH_3} = 3P^{o}_{PCl_3} - P'_{HCl} - 2P'_{P_2} - 4P'_{P_4} \qquad (22)$$

after P'_{HCl} has been calculated from

$$P'_{HCl} = 3AP^{o}_{PCl_3}/(A+K_4) \quad , \qquad (23)$$

where

$$A = P'^{(1-y')x'/2}_{P_2} \; P'^{(1-y')(1-x')/4}_{P_4} \; P'^{y'}_{PH_3} \; P'^{.5(1-3y')}_{H_2} \qquad (24)$$

and y' has been found using eq. (19). The fraction of the phosphorus in the vapor phase, v, then is

$$v = (2P'_{P_2} + 4P'_{P} + P'_{PH_3})/P^{o}_{PCl_3} \quad . \qquad (25)$$

To determine the equilibrium partial pressures in the deposition zone of the hydride system, a value of P_{P_4} is assumed. P_{P_2} and x can then be calculated using eqs. (10) and (15). From a chlorine balance the decrease in the InCl pressure must equal the increase in the HCl pressure so that

$$P_{InCl} = P_{InCl^1} + P_{HCl^1} + P_{HCl^2} - P_{HCl} = R - P_{HCl} \quad . \qquad (26)$$

The phosphorus balance yields

$$P_{PH_3} = P_{PH_3^2} - 2P_{P_2} - 4P_{P_4} - (P_{HCl} - P_{HCl^1} - P_{HCl^2}) \qquad (27)$$

where the term in the parentheses is the amount of InP deposited. The hydrogen pressure is

$$P_{H_2} = 1 - P_{P_2} - P_{P_4} - P_{PH_3} - P_{InCl} - P_{HCl}$$

$$= 1 + P_{P_2} + 3P_{P_4} - P_{PH_3}^2 - P_{InCl^1} - 2P_{HC^1} - 2P_{HCl^2} + P_{HCl}$$

$$= S + P_{HCl} \qquad (28)$$

Noting that $P_{H_2} \simeq S$, P_{PH_3} can be computed using eq. (16). From the deposition reaction

$$K_{4r} = P_{HCl}/(P_{InCl}\, P_{H_2}^{.5(1-3y)}\, P_{P_2}^{(1-y)x/2}\, P_{P_4}^{(1-6)(1-x)/4}\, P_{PH_3}^{y})$$

$$= P_{HCl}/(R-P_{HCl})A \qquad (29)$$

or

$$P_{HCl} = RAK_{4r}/(1+AK_{4r}) \qquad (30)$$

The substript $4r$ is used to designate the fact that the deposition reaction is the opposite of reaction (4). P_{InCl} can now be computed using eq. (26) and P_{PH_3} can be checked with eq. (27).

For the chloride process $3P_{PCl_3^2}$ is substituted for P_{HCl^2} in eqs. (26-28) since downstream PCl_3 is used instead of HCl. Also, $P_{PCl_3^o}$ must be substituted for $P_{PH_3^2}$ in the phosphorus balance equation, eq. (27), and in eq. (28).

The ideal growth rate, r, is

$$r = \frac{P_{InCl^1} - P_{InCl}}{P_{InCl^1}} \times \frac{\text{no. of } InCl^1 \text{ atoms crossing unit area per unit time}}{\text{no. of In atoms per unit volume in InP}}$$

Therefore,

$$r \propto P_{InCl^1} - P_{InCl} \qquad (31)$$

when the cross sectional area of the growth tube and the total flow rate are held constant.

3. Results

a. Source Zone

The fraction of the phosphorus, u, consumed by its reaction with liquid indium, and the fraction of the InP, v, consumed by the three units of HCl generated from one unit of PCl_3, are plotted as a function of the PCl_3 partial pressure in figure 17. u varies considerably as it is .19 when $P_{PCl_3^o}$ = .001 atm. and is .99 when $P_{PCl_3^o}$ = .1 atm. However, about 96% of the HCl reacts with the InP over the entire range as v decreases from 2.94 at $P_{PCl_3^o}$ = .001 to 2.86 at $P_{PCl_3^o}$ = .1 atm. The percent of the HCl consumed by its reaction with liquid indium is also almost constant as w varies from .988 when P_{HCl^o} = .003 to .990 when P_{HCl^o} = .3 atm. The variation of v and w is small primarily because the number of moles of gas present during the reactions remains essentially constant.

The prediction that the InP crust does not completely cover the liquid indium is in disagreement with observations made on the chloride growth of the related compound, GaAs, [38-39] unless it can be shown that a portion of the crust is $GaCl_3$. However, this analysis can explain why the crust nucleates at the downstream end of the boat, [38] there is an abrupt change in the carrier concentration in InP films when the HCl flow rate is changed [8,18,19] and this transient behavior has a longer time constant when a larger boat is used [8]. Nucleation occurs at the upstream end where the HCl concentration is less due to the fact that much of it has been removed by reaction with the indium. If the HCl concentration

Fig. 17. The fraction, u, of phosphorus consumed by the reaction with liquid indium, and the fraction, v, of the InP consumed by the reaction with HCl plotted as a function of source input PCl_3.

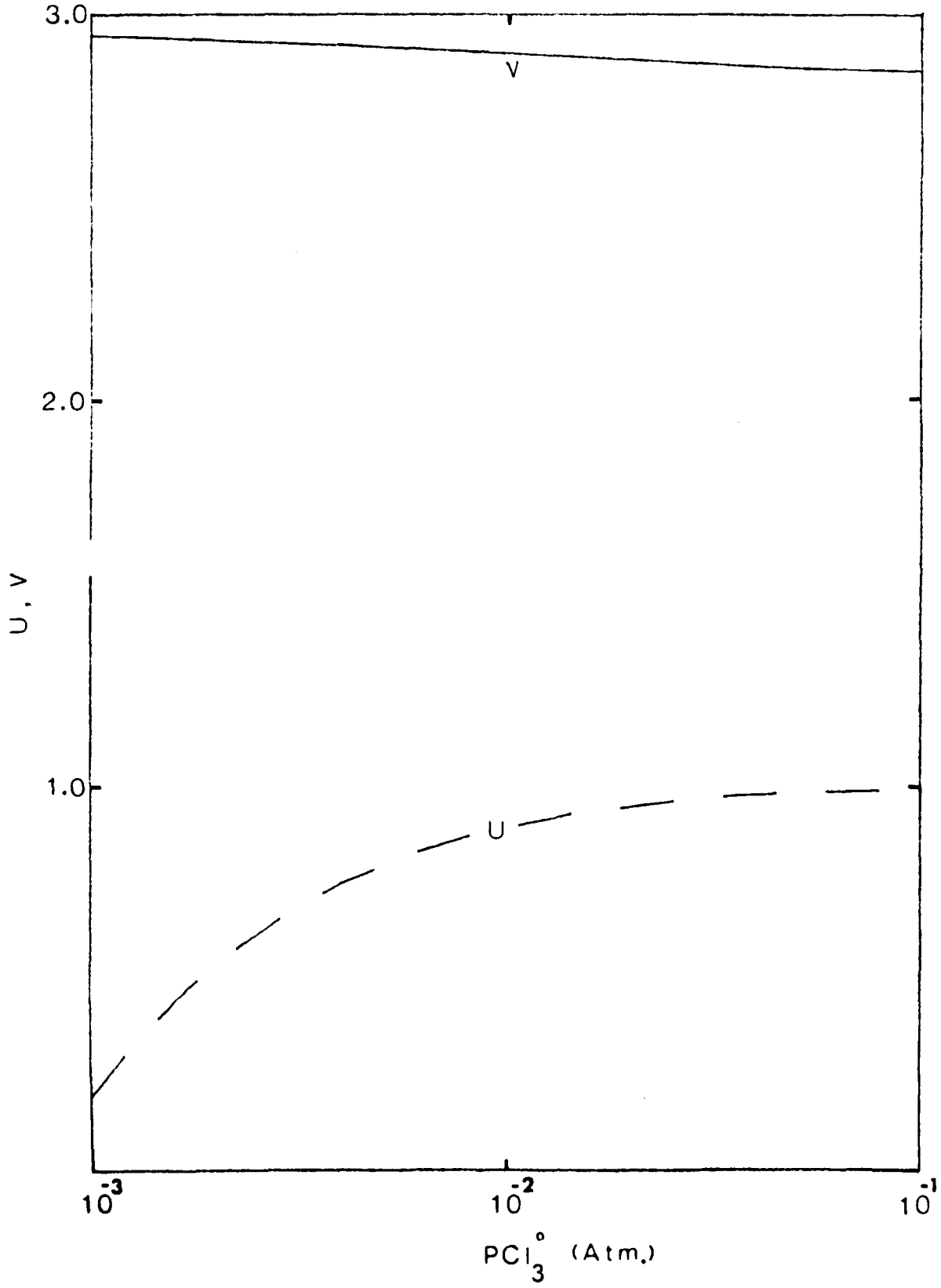

is less, the newly formed InP crust will be attacked at a slower rate. The abrupt change in the carrier concentration is due to a change in the steady state distribution of InP crust and exposed liquid indium, and the transient is longer when a larger boat is used because it takes a longer time to reach the new steady state distribution.

b. HCl Concentration

The equilibrium partial pressures in the deposition zone are plotted as a function of $HCl^o/3$, PH_3^2, and PCl_3^o respectively in figures 18a,b and c. In figure 18a the HCl pressure increases almost linearly from $.319 \times 10^{-3}$ when $P_{HCl^o} = .003$ to 12.3×10^{-3} when $P_{HCl^o} = .3$ atm. This behavior is due to the almost constant 99% conversion efficiency of the HCl in the source zone. The small negative deviation from linearity is due to the consumption of phosphorus. As the phosphorus is used up, the driving force for deposition, in which HCl is generated (eq. 4), is reduced. In fact, this effect dominates at the highest HCl^o pressures where the HCl curve becomes more sublinear.

In addition to the decreasing partial pressures of the phosphorus containing compounds in figure 18a there is an almost linear increase in the InCl concentration. Again, this can be attributed to the almost constant HCl conversion efficiency in the source zone.

That increasing the deposition of InP increases the HCl concentration is shown more vividly in figure 18b where the constituent partial pressures are plotted as a function of the input PH_3 pressure. P_{HCl^o} is held constant at .03 atm., yet P_{HCl} increases from 1.12×10^{-3} to 4.74×10^{-3} atm. as the driving force for InP deposition increases with the increase in $P_{PH_3^2}$ from .001 to .1 atm. The increased deposition is also, of course, reflected in a slowly decreasing InCl concentration from 28.9×10^{-3} to 25.3×10^{-3} atm.

Fig.18(a). The deposition zone equilibrium constituent partial pressures plotted as a function of the HCl input pressures.

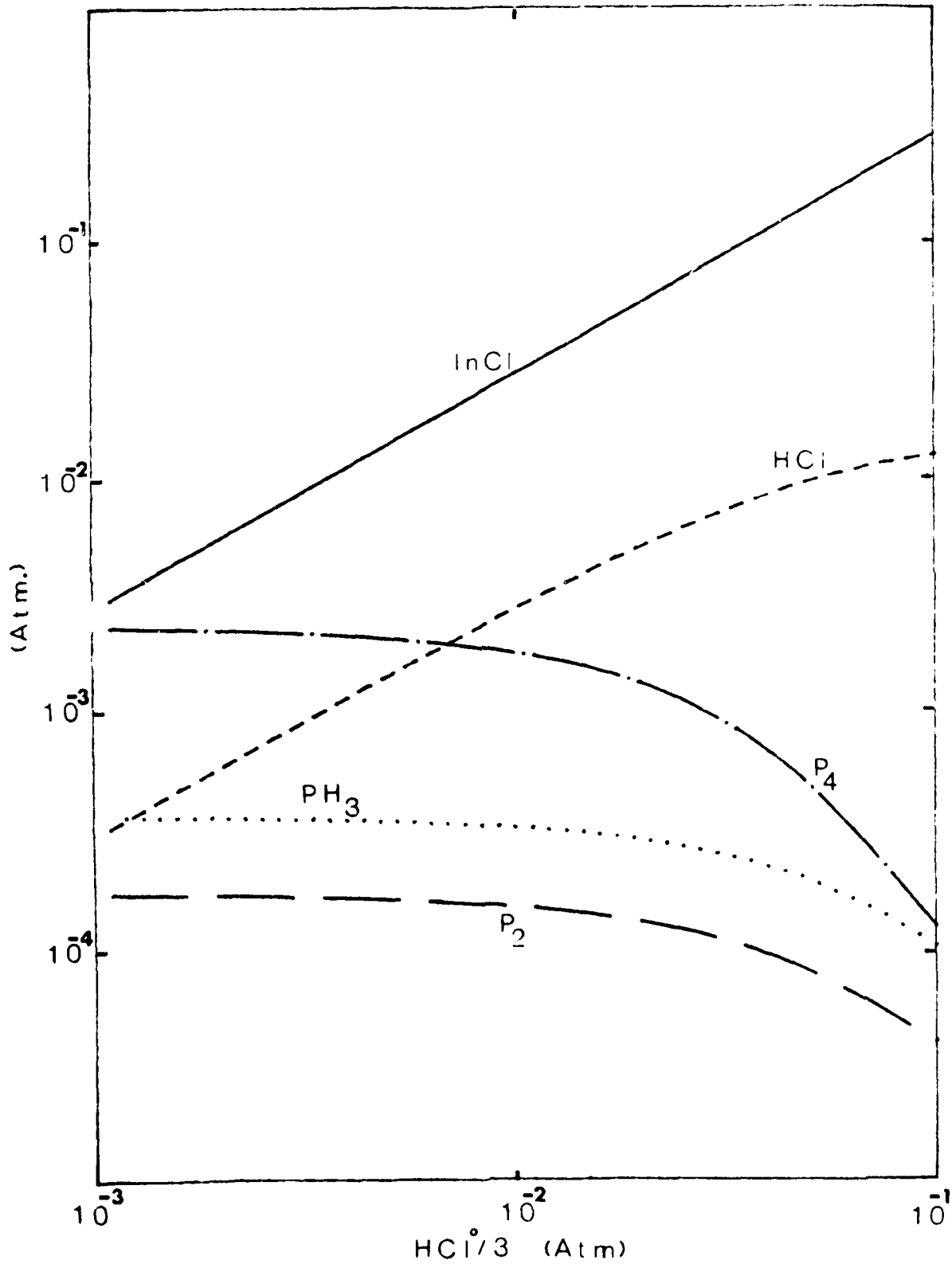

Fig. 18(b). The deposition zone equilibrium constituent partial pressures plotted as a function of the PH_3 input pressures.

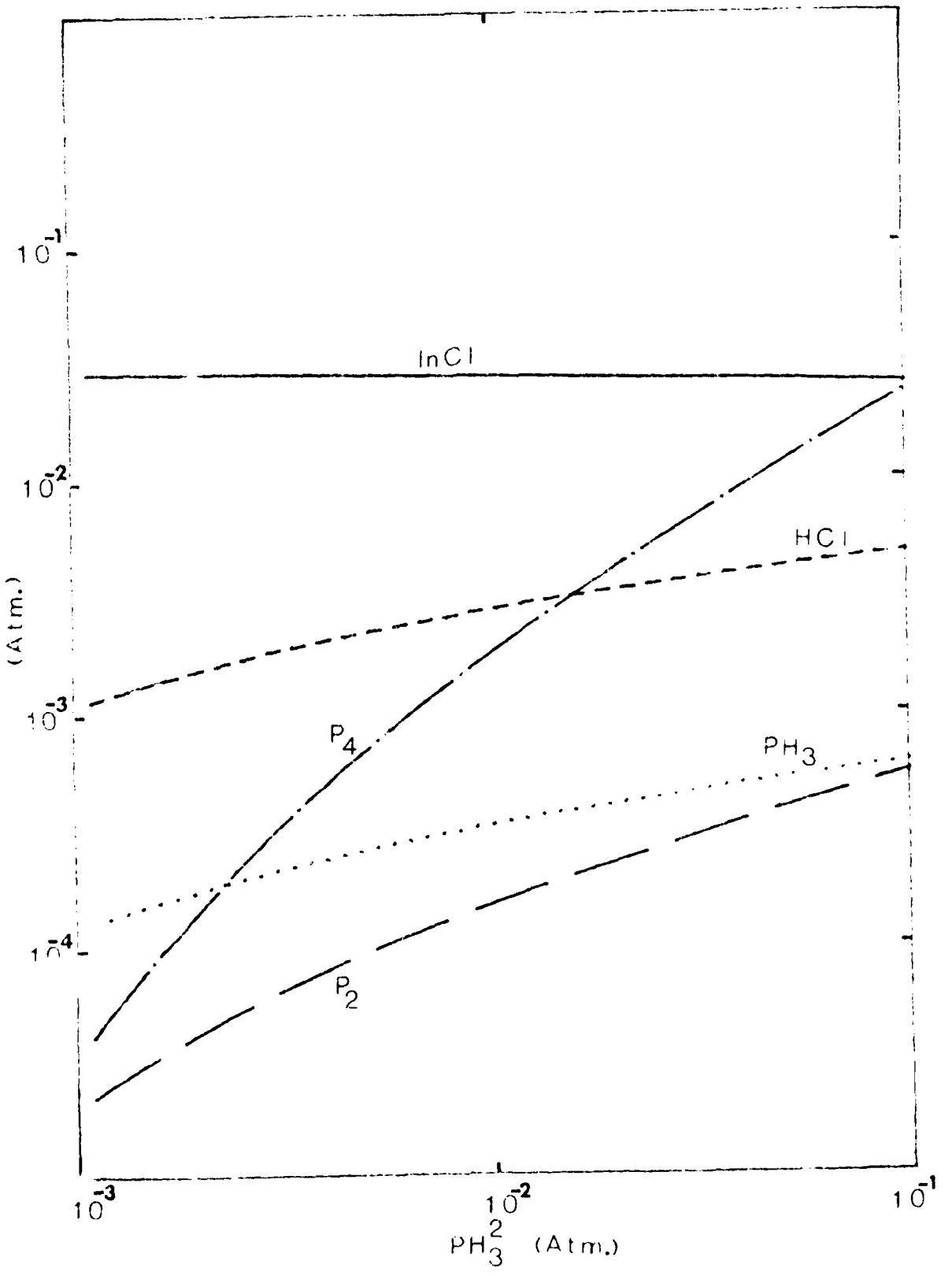

Fig.18(c). The deposition zone equilibrium constituent partial pressures plotted as a function of the PCl_3 input pressures.

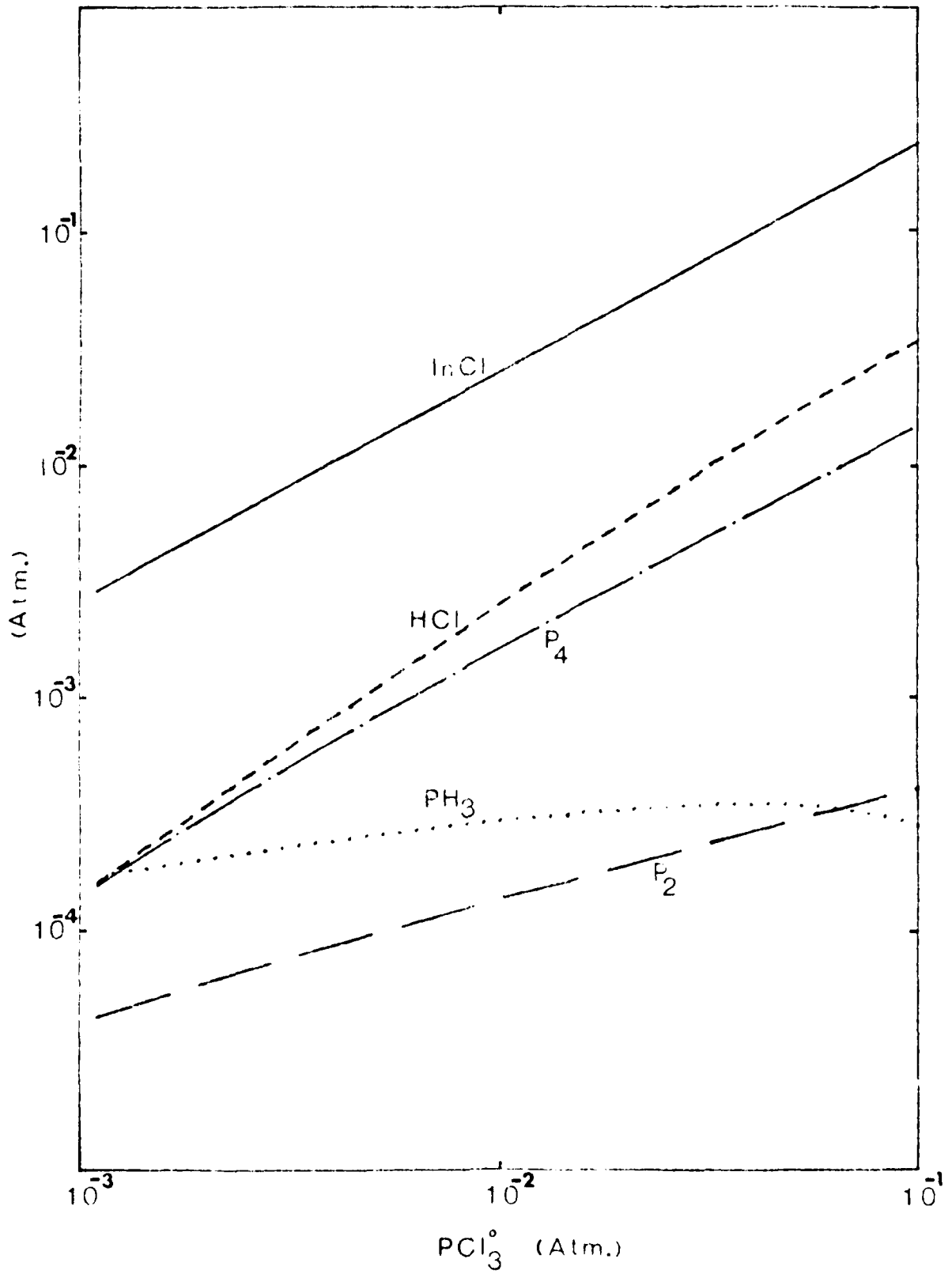

Clearly, all of the additional phosphorus is not consumed by the deposition reaction so that the partial pressures of P_2, P_4 and PH_3 increase with increasing $P_{PH_3^o}$. In fact, the amount of phosphorus in the vapor increases substantially because the larger phosphorus pressures do not increase the supersaturation as much as the larger HCl pressures do. This is why P_{InCl} is not reduced as much by raising $P_{PH_3^o}$ as $P_{(P_2,P_4,PH_3)}$ are reduced by raising P_{HCl^o}.

There appears to be no thermodynamic basis for InP being p-type when the V/III ratio exceeds 1/3 [8]. Thus, the chloride growth of the p-type films by injecting PCl_3 downstream must have a kinetic basis.

The effects of varying the PCl_3^o concentration is a limited combination of the effects of separately varying the HCl^o and PH_3^o pressures; the limitation is due to the V/III ratio being fixed. The rate of increase of the HCl pressure - the HCl pressure at PCl_3^o = .001 atm. is $.175 \times 10^{-3}$ atm. and is 37.2×10^{-3} atm. at PCl_3^o = .1 atm. - is larger than it is when the HCl^o pressure is varied because both the increasing InCl and increasing phosphorus pressures contribute to increasing the InP deposition. For the same reason the InCl pressures are less than they are when HCl^o is varied, and the P_2, P_4 and PH_3 pressures are less than when PH_3^o is varied.

The theoretical silicon activities corresponding to the PCl_3^o pressures of 2×10^{-3} and 2×10^{-2} atm. are 2×10^{-6} and 7×10^{-8}.[12] Thus the almost two orders of magnitude change in the background carrier concentration observed by changing the PCl_3^o pressure between these two limits [8,17,18] can be explained thermodynamically. Also, the lower background carrier concentrations in chloride grown films [7-8,17-19] could have a thermodynamic basis since typical PCl_3^o pressures are .01-.02 atm.,

whereas typical HCl^{o} and PH_3^{2} pressures are .01 atm. [6]. The three to six fold larger HCl pressure in the chloride system cannot, however, completely account for the difference in the background carrier concentrations. Therefore, such factors as the purity of the HCl and the slow decomposition of the PH_3 [9,10] must be considered.

Fairhurst et al[7] have attributed the slow decomposition of PH_3 to the large variation in the background carrier concentration when films are grown under similar conditions. The thermodynamic calculations show that only 4% of the phosphorus is in the form of PH_3 at normal operating conditions, and it has not been shown that PH_3 is an intermediate during the formation of P_2 or P_4 from the decomposition of PCl_3. It, therefore, seems more likely that the variation in the background carrier concentration is due to other factors.

It would appear that the deposition zone HCl concentration could be greatly increased by introducing HCl or PCl_3 downstream from the indium boat. However, introducing HCl by itself is not as effective as it first might seem because it reverses the deposition reaction. For every HCl molecule introduced there is almost one less 'molecule' of InP deposited. Thus, there is very little change in the deposition zone HCl concentration, and this is depicted in figure 19 where the HCl concentration is plotted as a function of the downstream input HCl (HCl^{2}) pressure for the hydride system or PCl_3 (PCl_3^{2}) pressure for the chloride system. The range of HCl values are also listed in table 4 for three different values of $HCl^{o}/3$, PH_3^{2}, and PCl_3^{o}.

The range is determined by the amount of HCl^{2} or PCl_3^{2} it takes to completely reverse the deposition reaction - that is, the concentration above which etching occurs. At the highest HCl^{o}, PH_3^{2}, and PCl_3^{o} the

Fig. 19. The equilibrium HCl concentration plotted as a function of downstream HCl/3 or PCl_3, when the input HCl/3 (--), PH_3 (---), or PCl_3 (···) pressure equals .01/3, .01, and .03 atm.

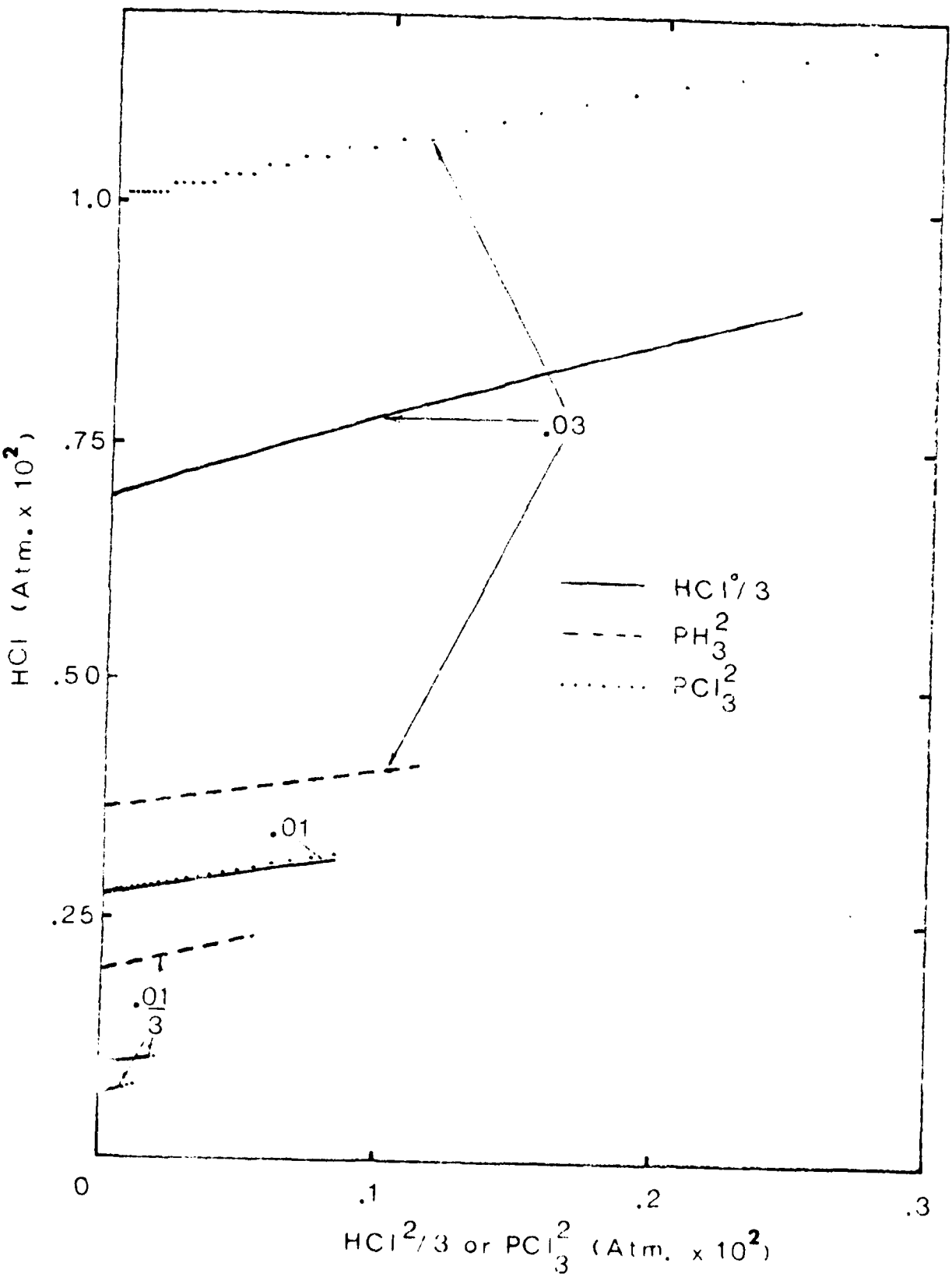

range is smallest for PH_3^2 and largest for PCl_3^o for reasons given above. That is, PH_3 increases the supersaturation the least so it can be reduced to zero with less HCl^2, and PCl_3^o increases the supersaturation the most since both the InCl and phosphorus pressures are increased.

At normal operating conditions - $HCl^o/3$, PH_3^2 and PCl_3^o = .01 atm. - the HCl concentration is increased only about 10%. This only decreases the theoretical silicon activity by about the same amount so it does not appear to be an effective way to reduce the background carrier concentration. Kennedy et al [40] did attempt to reduce the carrier concentration in hydride grown GaAs films by introducing HCl downstream, and they were unsuccessful.

c. Growth Rate

A normalized growth rate, which is proportional to the difference between the deposition zone input and output InCl pressures, is plotted in figure 20 as a function of $HCl^o/3$, PH_3^2 and PCl_3^o. For the hydride system it is seen that the growth rate increases more rapidly with HCl^o than with PH_3^2. This, again, can be attributed to the greater sensitivity of the supersaturation to the HCl^o pressure.

Detailed studies of the effects of HCl^o and PH_3^2 on the growth rate of InP have not been made, but similar studies have been made for GaAs [9,41]. Both Enstrom et al [9] and Shaw [41] found that the growth rate initially increases rapidly with HCl^o, and it increases more slowly with AsH_3^2 as one would predict thermodynamically. However, the growth rate reaches a peak and then decreases as HCl^o becomes larger. Shaw [42,43] attributes this to the poisoning of surface sites by GaCl. An alternative explanation is that once the supersaturation exceeds a certain value, GaAs nucleation occurs on the side walls. The measured growth rate on the substrate then decreases because the supersaturation is reduced by deposition on the side walls.

Fig. 20. The normalized ideal growth rate plotted as a function of input HCl/3, PH_3 and PCl_3 pressures.

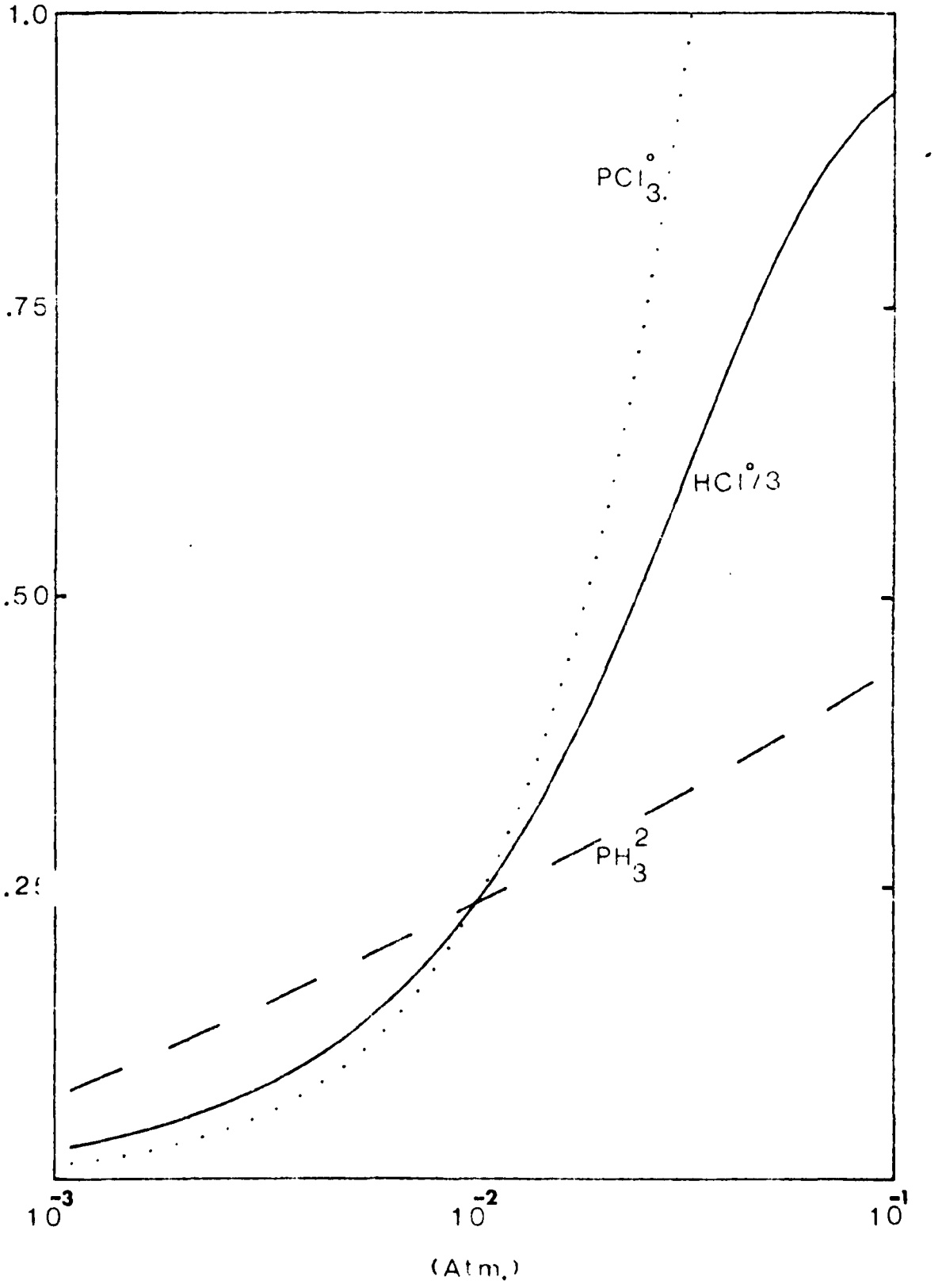

TABLE 4

	.01/3	.01	.03
$HCl^{\circ}/3$	.990 - 1.06	2.76 - 3.14	6.92 - 8.97
PH_3^2	1.97 - 2.23	"	3.66 - 4.14
PCl_3	.756 - .808	2.77 - 3.20	10.0 - 12.3

The range of HCl pressures x 10^3 in the deposition zone generated by introducing HCl or PCl_3 downstream at concentrations of 0 and the point where etching begins for input HCl/3, PH_3 or PCl_3 pressures of .01/3, .01, and .03 atms.

TABLE 5

	.01/3	.01	.03
$HCl^{\circ}/3$	.093	.092	.091
PH_3^2	.192	"	.041
PCl_3°	.069	.091	.123

The HCl^2/HCl°, $HCl^2/3/PH_3^2$ and PCl_3^2/PCl_3° ratios at the concentration where etching begins for input HCl/3, PH_3 or PCl_3 pressures of .01/3, .01 and .03 atms.

Zinkiewicz et al [6] have observed that increasing the H_2 flow rate while holding the partial pressures of PH_3^2 and HCl^o constant reduces the growth rate. This is, of course, the opposite of what one would predict - the growth rate should increase linearly with the flow rate since the supersaturation is unchanged. A possible explanation is that the reaction between the liquid indium and the HCl is incomplete [44], and the larger HCl concentration in the deposition zone retards the deposition reaction. The same authors also observed that increasing the H_2 flow rate while keeping the HCl^o and PH_3^2 flow rates constant resulted in an increased growth rate. On the basis of thermodynamics one would predict that the growth rate should be reduced since the supersaturation is reduced. The larger growth rate has been attributed to the slow PH_3 decomposition and a more efficient reaction between InCl and PH_3 than between InCl and P_4 or P_2[6].

If thermodynamics determined the growth rate, the rate should increase the most rapidly with the PCl_3^o pressure because the supersaturation increases the most rapidly. However, Clarke and Taylor found that the growth rate saturates at about .2μ/min, [19] which is an order of magnitude less than the maximum value found by Zinkiewicz et al [6] using the hydride technique. As stated above, this has been attributed to the larger amount of undissociated PH_3 in the hydride system.

The degree to which the downstream HCl or PCl_3 thermodynamically retards the deposition process is illustrated in figure 21 where the normalized growth rates are plotted as a function of $HCl^2/3$ or PCl_3^2. The HCl^2/HCl^o and PCl_3^2/PCl_3^o ratios at the point when etching begins for $HCl^o/3$, PH_3^2 and PCl_3^o = .01/3, .01, and .03 atm. are listed in Table 4. The ratio decreases with increasing PH_3^2, is essentially constant for increasing HCl^o, and increases with increasing PCl_3^o. These trends can

Fig. 21. The normalized ideal growth rate plotted as a function of downstream HCl/3 or PCl_3 input pressures when the input HCl/3, PH_3 or PCl_3 pressure equals .01/3, .01, and .03 atm.

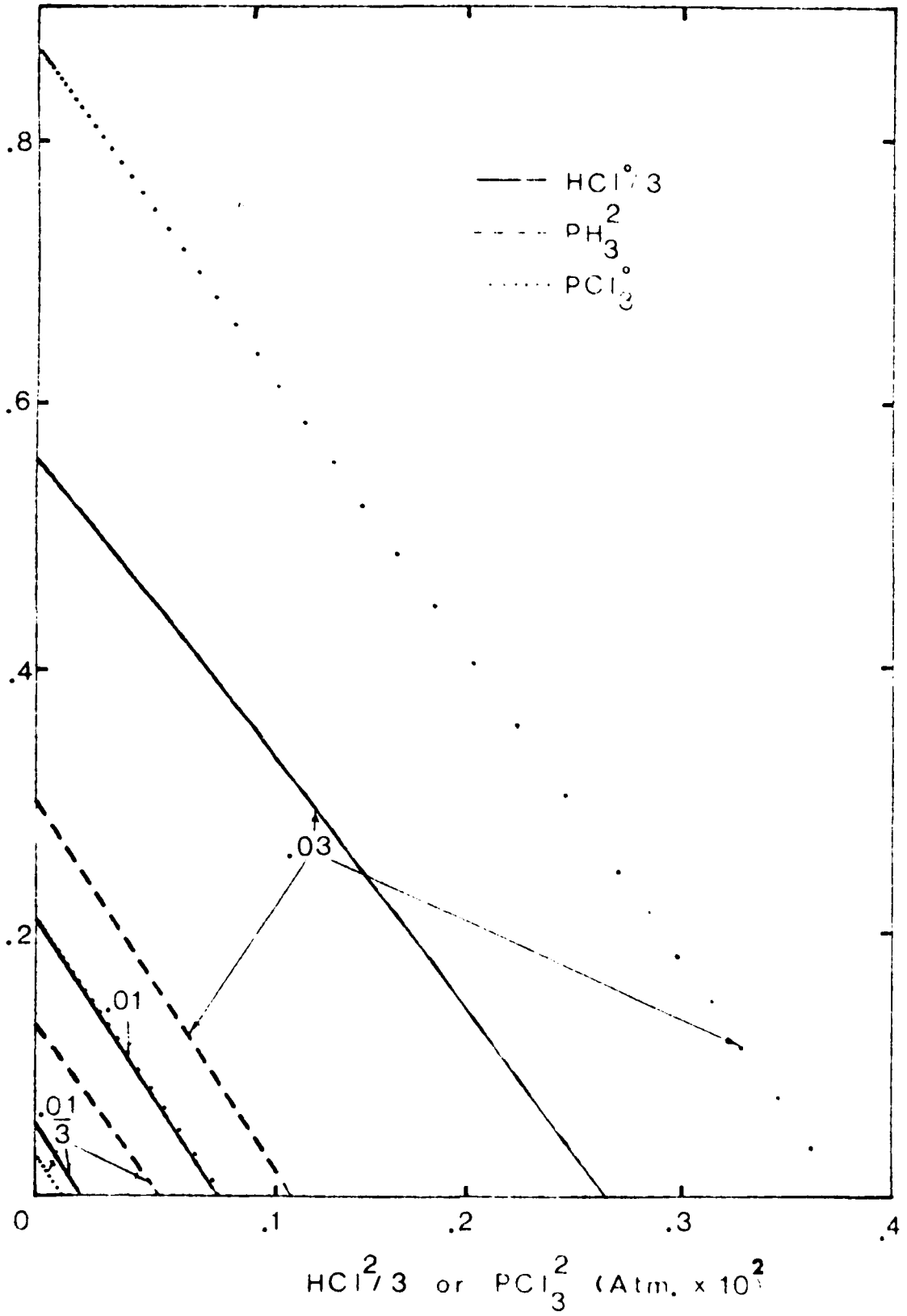

B. Thermodynamic Effects of Using an Inert Gas

Hydrogen is an excellent carrier gas because it can be highly purified at a relatively low cost using a hydrogen purifier. It also getters oxygen. Recently, some people have suggested using N_2 as the carrier gas because it can be highly purified by first liquifying it [19]. One should consider the possibility of forming nitrides if he chooses to use N_2, but he should also consider how substituting an inert gas for the H_2 affects the thermodynamics of the growth process. The latter consideration is the topic of this communication.

The parameters considered in this paper are the thermodynamic growth rate, and the equilibrium PH_3 and HCl concentrations in the growth zone. Clearly, reducing the H_2 partial pressure will reduce the PH_3 pressure. This is important since it has been suggested that the growth rate is higher when more PH_3 is present due to the fact that InCl more readily reacts with PH_3 than with P_2 or P_4 [8]. (It should be noted that PH_3 decomposes rather slowly [20,21] so that more PH_3 is present in the growth zone than is computed from thermodynamic data. Thus, the calculations that follow can only be used to indicate the trends). Knowing the HCl concentration is important because it is thought that increasing the HCl concentration reduces the activity of silicon in the quartz reactor.

From the deposition reaction,

$$InCl + (1-y)\frac{x}{2}P_2 + (1-y)\frac{(1-x)}{4}P_4 + yPH_3 + \frac{1}{2}(1-3y)H_2 \rightarrow InP(s) + HCl \quad , \qquad (4)$$

one can see that reducing the H_2 pressure will reduce the deposition rate, and this, in turn, will reduce the HCl partial pressure since it is formed during the deposition reaction. In this equation x is the ratio of the amount of phosphorus in the P_2 form to the amount of phosphorus in the P_2 and P_4 form and is given by the equation,

$$x = \frac{P_{P_2}}{P_{P_2} + 2P_{P_4}} \quad . \tag{4}$$

y is the fraction of the phosphorus in PH_3 and is given by,

$$y = \frac{P_{PH_3}}{P_{PH_3} + xP_{P_2} + (1-x)P_{P_4}} \quad . \tag{5}$$

First, the output pressures from the source zone, designated by the superscript, 1, must be determined for the source zone reaction

$$HCl + In(s) \rightarrow InCl + \frac{1}{2} H_2 \quad . \tag{1}$$

The output InCl pressure is, from a chlorine balance,

$$P_{InCl}^{1} = P_{HCl}^{o} - P_{HCl}^{1} \tag{5}$$

where P_{HCl}^{o} is the input HCl pressure. P_{HCl}^{1} can be found from the equation

$$P_{HCl}^{1} = \frac{P_{HCl}^{o}(1 - P_{HCl}^{o})^{1/2}}{(1 - P_{HCl}^{o})^{1/2} + K_5} \tag{7}$$

$$P_{H_2} = 1 - P_{HCl}^{o} \tag{6}$$

was used in deriving eq. (7).

For the deposition zone first a value of P_{P_4} is assumed, and then it is used to determine P_{P_2} after the equilibrium constant for the reaction

$$P_2 \rightarrow \frac{1}{4} P_4 \tag{3}$$

has been found. P_{PH_3} can be found from the phosphorus balance,

$$P_{PH_3} = P_{PH_3^o} - 2P_{P_2} - 4P_{P_4} - (P_{HCl} - P_{HCl^I}) \quad , \tag{27}$$

where $P_{PH_3^o}$ is the input phosphine pressure and $P_{HCl} - P_{HCl^I}$ is the amount of phosphorus consumed by the reaction with InP. Again, P_{InCl} is found from the chlorine balance

$$P_{InCl} = P_{InCl^I} + P_{HCl} - P_{HCl^I} \quad . \tag{28}$$

The total pressure is I atm, so that

$$\begin{aligned} P_{H_2} &= 1 - P_{InCl} - P_{P_2} - P_{P_4} - P_{PH_3} - P_I - P_{HCl} \\ &= 1 - P_{HCl^I} - 2P_{HCl^I} + P_{P_2} + 3P_{P_4} - P_{PH_3^o} - P_I + P_{HCl} \\ &= S + P_{HCl} - P_I \quad , \end{aligned} \tag{29}$$

where P_I is the partial pressure of the inert gas. Now, P_{PH_3} can be computed from

$$P_{PH_3} = P_{P_2}^{x/2} P_{P_4}^{(1-x)/4} P_{H_2}^{3/2} / K_{13} \quad , \tag{31}$$

where K_{13} is the equilibrium constant for the dissociation reaction

$$PH_3 \rightarrow \frac{x}{2} P_2 + \frac{(1-x)}{4} P_4 + \frac{3}{2} H_2 \quad . \tag{32}$$

P_{HCl} can be calculated from

$$P_{HCl} = \frac{RK_1^Q}{1 + K_1^Q} \quad , \tag{30}$$

$$Q = P_{P_2}^{(1-y)x/2} P_{P_4}^{(1-y)(1-x)/4} P_{PH_3}^{-1} P_{H_2}^{1/2(1-3y)} \qquad (12)$$

K_1 is the equilibrium constant for the deposition reaction, and K is defined in eq. (10). Finally, P_{PH_3} computed from eq. (9) is compared with the value found from eq. (13). If they are not the same, a new value of P_{P_4} is assumed. The process is repeated until the two P_{PH_3} values are equal.

The thermodynamic growth rate, R, is

$$R = \frac{P_{InCl}^{I} - P_{InCl}}{P_{InCl}^{I}} \times \frac{\text{no. of } InCl^{I} \text{ atoms crossing unit area per unit time}}{\text{no. of In atoms per unit volume in InP}} .$$

Therefore, $R = P_{InCl}^{I} - P_{InCl}$ (14)

Using the thermodynamic data collected by Shaw [25], the equilibrium partial pressures of HCl, PH_3, H_2, P_2, P_4 and InCl were computed and are plotted as a function of the inert gas partial pressure in figure 22. For these calculations the source temperature was, T_S = 750°C, the deposition temperature was, T_D = 650°C, and both P_{HCl}^{o} and $P_{PH_3}^{o}$ were .01 atm. P_{HCl} decreases by about a factor of 10 as P_I increases from 0 to .98 atm. This reduction is due to less hydrogen being available to form HCl during the deposition reaction. Because there is less InP deposited with increasing P_I, P_{InCl} increases. P_{PH_3} decreases two orders of magnitude over the range of P_I since there is less hydrogen available, and as a result P_{P_2} and P_{P_4} increase. They also increase because there is less InP deposited.

That there is less deposition when P_I increases is shown in figure 23 where the ideal growth rate is plotted vs P_I. R decreases continuously until at P_I = .975 atm there is no deposition. The effects on the growth rate of decreasing P_{HCl}^{o} or $P_{PH_3}^{o}$ by one third, increasing P_{HCl}^{o} or $P_{PH_3}^{o}$

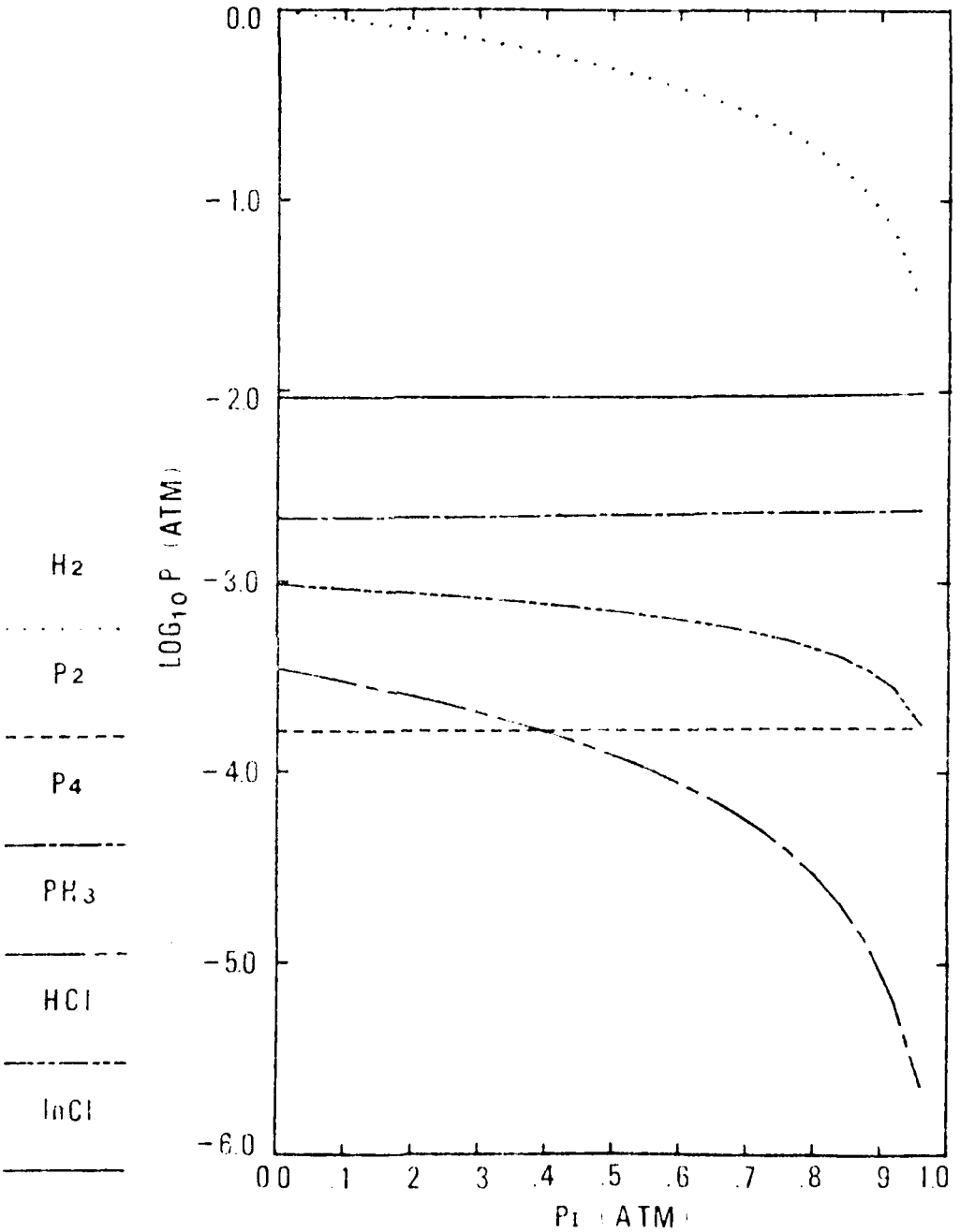

Figure 27. The equilibrium partial pressures of HCl, PH_3, P_2, P_4, InCl, and H_2 in the deposition zone plotted as a function of P_I when P°_{HCl} and $P^{\circ}_{PH_3}$ = .01 atm., T_S = 750°C, and T_D = 650°C.

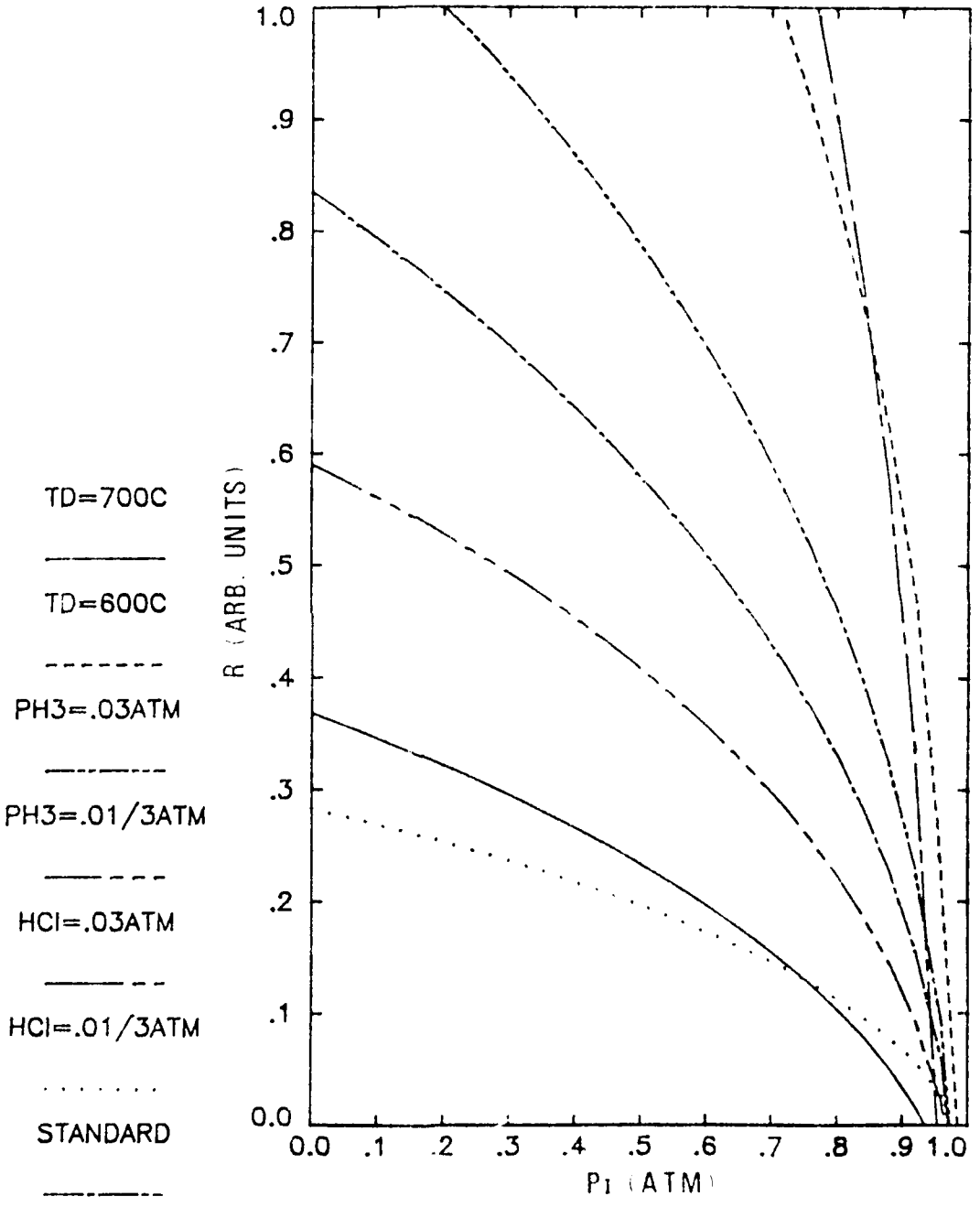

Figure 7. The thermodynamic growth rate plotted as a function of P_I when the $P_{HCl}^o/P_{PH_3}^o$ ratio is .01/3/.01, .01/.01, .03/.01, .01/.01/3 or .01/.03 and when T_D = 600 and 700°C.

by a factor of three, or increasing or decreasing T_D by 50°C are also shown in figure 13. The effects are largest when $P_I = 0$, and all of the curves tend to converge on the point $R = 0$ and $P_I = .97$.

Reducing P_{HCl^o} by one third, reduces the initial growth rate by one third, and tripling P_{HCl^o} triples the initial growth rate. $R \propto P_{HCl^o}$ in this range because $P_{InCl^1} \propto P_{HCl^o}$ and $R \propto P_{InCl^1}$. The effect of thirding or tripling $P_{PH_3^o}$ is smaller as it only changes the initial growth rate by 30%. Adding to or reducing the PH_3^o concentration has a smaller effect because the free energy change for the deposition reaction is much more sensitive to the HCl concentration. Lowering the deposition temperature by 50°C doubles the initial growth rate and raising it by 50° halves the growth rate. These effects reflect the temperature dependence for the deposition reaction.

How changing HCl^o, PH_3^o, and T_D affects the equilibrium HCl and PH_3 concentrations for different values of P_I is illustrated in table 6.

That decreasing the hydrogen partial pressure decreases the growth rate has been verified experimentally for the chloride growth of GaAs, InAs, GaP, and InP [45]. The investigators also found that there were kinetic, as well as thermodynamic, effects such as the growth rate being reduced more by a heavier inert gas.

	P_I (atm.)	0	.1	.2	.3	.4	.5	.6	.7	.8	.9
	$\frac{P_{HCl^o}}{P_{PH_3^o}}$										
$P_{HCl} \times 10^4$ atm.	.01/3/.01	3.23	3.08	2.93	2.76	2.57	2.36	2.13	1.86	1.53	1.08
	.01/.01	9.53	9.10	8.64	8.13	7.59	6.97	6.28	5.47	4.48	3.11
	.03/.01	27.10	25.92	24.63	23.23	21.67	19.92	17.91	15.52	12.52	8.15
	.01/.01/3	7.08	6.78	6.45	6.10	5.70	5.25	4.74	4.14	3.40	2.38
	.01/.03	12.38	11.82	11.22	10.56	9.85	9.05	8.15	7.09	5.78	3.97
$P_{PH_3} \times 10^4$ atm.	.01/3/.01	3.55	3.04	2.55	2.08	1.65	1.26	.896	.578	.311	.105
	.01/.01	3.46	2.96	2.48	2.03	1.61	1.22	.864	.554	.292	.093
	.03/.01	3.20	2.73	2.28	1.86	1.47	1.10	.775	.484	.242	.062
	.01/.01/3	2.51	2.16	1.81	1.49	1.19	.903	.683	.416	.221	.072
	.01/.03	4.62	3.94	3.29	2.68	2.12	1.00	1.13	.717	.372	.113
$P_{HCl} \times 10^4$ atm.	T_D										
	600	18.81	18.07	17.26	16.37	15.38	14.26	12.97	11.42	9.48	6.72
	650	9.53	9.10	8.64	8.13	7.59	6.97	6.28	5.47	4.48	3.11
	700	4.87	4.63	4.38	4.12	3.82	3.45	3.14	2.72	2.21	1.52
$P_{PH_3} \times 10^4$ atm.	600	3.84	3.28	2.75	2.26	1.79	1.36	.967	.621	.329	.105
	650	3.46	2.96	2.48	2.03	1.61	1.22	.864	.554	.292	.093
	700	3.10	2.64	2.21	1.81	1.43	1.08	.769	.492	.260	.083

Table 6. The HCl and PH_3 partial pressures for different values of P_I for standard conditions, when P_{HCl^o} or $P_{PH_3^o}$ = .01/3 or .03 atm., or when T_D = 600 or 700°C.

References

[1] G. B. Stringfellow, Ann. Rev. Mater. Sci. 8 (1978) 73.

[2] P. Vohl, J. Crystal Growth 54 (1981) 101.

[3] H. M. Manasevit and W. T. Simpson, J. Electrochem. Soc. 118 (1971) C291; 120 (1973) 135.

[4] B. I. Miller, J. H. McFee and K. J. Bachmann, J. Electrochem. Soc. 124 (1977) 259.

[5] R. Sankaran, G. A. Antypas, K. L. Moon, J. S. Escher and L. W. James, J. Vacuum Sci. Technol. 13 (1976) 932.

[6] L. M. Zinkiewicz, T. J. Roth, B. J. Skromme and G. E. Stillman, in: Proc. 8th Intern. Symp. on GaAs and Related Compounds, Vienna, 1980. Inst. Phys. Conf. Ser. 56 (inst. Phys. London, 1981 p. 19.

[7] K. Fairhurst, D. Lee, D. S. Robertson, H. T. Parfitt and W.H.E. Wilgoss, J. Mater. Sci. 16 (1981) 1013.

[8] R. C. Clarke, J. Crystal Growth 54 (1981) 88.

[9] R. E. Enstrom, C. J. Neuse, J. R. Appert and J. J. Gannon, J. Electrochem. Soc. 121 (1974) 1516.

[10] R. Fairman and R. Solomen, J. Electrochem. Soc. 120 (1973) 541.

[11] N. Susa, Y. Yamauchi and H. Kanbe, IEEE J. Quantum Electron. QE-16 (1980) 542.

[12] G. H. Olsen, C. J. Nuese and M. Ettenberg, IEEE J. Quantum Electron. QE-15 (1979) 688.

[13] H. H. Weider, A. R. Clawson, D. I. Elder, and D. A. Collins, IEEE Electron. Dev. Lett. EDL2, 73 (1981).

[14] B. K. Ridley, J. Appl. Phys. 48, 754 (1977).

[15] A. R. Clawson, D. A. Collins, D. I. Elder, and J. J. Monroe, Laboratory Procedures for Etching and Polishing InP Semiconductors, N.O.S.C. Technical Note 592, (1978).

[16] G. H. Olsen and M. Ettenberg, J. Appl. Phys. 45, 5112 (1974).

[17] R. C. Clarke, J. Crystal Growth 23, 166 (1974).

[18] R. C. Clarke and L. L. Taylor, J. Crystal Growth 31, 190 (1975).

[19] R. C. Clarke and L. L. Taylor, J. Crystal Growth 43, 473 (1978).

[20] R. H. Dalton, Proc. Roy. Soc. 128, 263 (1930).

[21] V. M. Donnelly and R. F. Karlicek, J. Appl. Phys. 53, 6399 (1982).

[22] D. W. Shaw, J. Crystal Growth 8, 117 (1971).

[23] K. A. Jones, J. Crystal Growth 60, 313 (1982).

[24] K. Ando, A. Yamamoto, and M. Yamaguchi, Jap. J. Appl. Phys. 20, 1107 (1981).

[25] D. W. Shaw, J. Phys. Chem. Solids 36, 111 (1975).

[26] Y. Yamauchi, N. Susa and H. Kanbe, J. Crystal Growth 56, 402 (1982).

[27] S. B. Hyder, R. R. Saxena, S. H. Chiao, and R. Yeats, Appl. Phys. Lett. 35, 787 (1979).

[28] H. Kanbe, Y. Yamauchi, and N. Susa, Appl. Phys. Lett. 35, 603 (1979).

[29] M. Glicksman, R. E. Enstrom, S. A. Mittleman, and J. R. Apert, Phys. Rev. B 9, 1621 (1974).

[30] S. B. Hyder, J. Electrochem. Soc. 123, 1503 (1976).

[31] S. B. Hyder, J. Crystal Growth 54, 109 (1981).

[32] N. Susa, Y. Yamauchi, H. Ando, and H. Kanbe, Jap. J. Appl. Phys. 19, L17 (1979).

[33] G. Beuchet, M. Bonnet, P. Thebault and J. P. Duchemin, J. Crystal Growth 57, 379 (1982).

[34] W. Y. Lum and A. R. Clawson, J. Appl. Phys. 50, 5296 (1979).

[35] A. R. Clawson, W. Y. Lum and G. E. McWilliams, J. Crystal Growth 46, 300 (1979).

[36] R. Bhat and S. K. Ghandhi, J. Electrochem. Soc. 125, 771 (1978); ibid 125, 1447 (1977).

[37] R. Bhat, B. J. Baliga and S. K. Ghandhi, J. Electrochem. Soc., 122, 1378 (1975).

[38] D. W. Shaw, J. Crystal Growth 8, 117 (1971).

[39] A. Boucher and L. Hollan, J. Electrochem. Soc. 117, 932 (1970).

[40] J. K. Kennedy, W. D. Potter and D. E. Davies, J. Crystal Growth 24/25, 233 (1974).

[41] D. W. Shaw, J. Electrochem. Soc. 117, 683 (1970).

[42] D. W. Shaw, J. Crystal Growth 8, 117 (1971).

[43] D. W. Shaw, J. Crystal Growth 31, 130 (1975).

[44] V. S. Ban, J. Crystal Growth 17, 19 (1972).

[45] O. Mizuno and H. Watanabe, J. Crystal Growth 30, 240 (1975).

END

FILMED

9-83

DTIC